



<https://technobius.kz/>

e-ISSN
2789-7338

Technobius

A peer-reviewed open-access journal

Technobius, LLP

Volume 4, No. 2, 2024



Technobius

Volume 4, No. 2, 2024



A peer-reviewed open-access journal registered by the Ministry of Culture and Information of the Republic of Kazakhstan, Certificate № KZ26VPY00087928 dated 21.02.2024

ISSN (Online): 2789-7338

Thematic Directions: Construction, Materials Science

Publisher: Technobius, LLP

Address: 2 Turkestan street, office 116, 010000, Astana, Republic of Kazakhstan

Editor-in-Chief:

   *Yelbek Utepov*, PhD, Professor, Department of Civil Engineering, L.N. Gumilyov Eurasian National University, Astana, Kazakhstan

Technical Editor:

   *Assel Tulebekova*, PhD, Professor, Department of Civil Engineering, L.N. Gumilyov Eurasian National University, Astana, Kazakhstan

Editors:

   *Victor Kaliakin*, PhD, Professor, Department of Civil & Environmental Engineering, University of Delaware, Newark, United States

   *Askar Zhussupbekov*, Doctor of Technical Sciences, Professor, Department of Civil Engineering, L.N. Gumilyov Eurasian National University, Astana, Kazakhstan

   *Talal Awwad*, Doctor of Technical Sciences, Professor, Department of Geotechnical Engineering, Damascus University, Damascus, Syria

   *Evgeniya Tkach*, Doctor of Technical Sciences, Professor, Department of Building Materials Science, Moscow State University of Civil Engineering, Moscow, Russian Federation

   *Ignacio Menéndez Pidal de Navascués*, Doctor of Technical Sciences, Professor, Department of Civil Engineering, Technical University of Madrid, Madrid, Spain

   *Irina Aubakirova*, Candidate of Technical Sciences, Associate Professor, Department of Building Materials Technology and Metrology, Saint Petersburg State University of Architecture and Civil Engineering, Saint Petersburg, Russian Federation

   *Daniyar Akhmetov*, Doctor of Technical Sciences, Associate Professor, Department of Construction and Building materials, Satbayev University, Almaty, Kazakhstan

   *Zhanbolat Shakhmov*, PhD, Associate Professor, Department of Civil Engineering, L.N. Gumilyov Eurasian National University, Astana, Kazakhstan

   *Timoth Mkilima*, PhD, Lecturer, Department of Environmental Engineering and Management, the University of Dodoma, Dodoma, Tanzania

   *Aliya Aldungarova*, PhD, Associate Professor, School of Architecture, Civil Engineering and Energy, D. Serikbayev East Kazakhstan Technical University, Ust-Kamenogorsk, Kazakhstan

Copyright: © Technobius, LLP

Contacts: Website: <https://technobius.kz/>
E-mail: technobius.research@gmail.com

CONTENTS

Title and Authors	Category	No.
Mineral powder based on basalt insulation waste for asphalt concrete <i>Duman Dyusembinov, Rauan Lukpanov, Adiya Zhumagulova, Assel Jexembayeva, Beksultan Chugulyov</i>	<i>Materials Science</i>	0056
Experimental study of sound wave propagation patterns <i>Alisher Imanov, Aigul Kozhas, Assel Mukhamejanova, Aida Nazarova, Dias Kazhimkanuly</i>	<i>Construction</i>	0057
Alkali-activated composites with synthetic fibers and recycled aggregates: a study of mechanical properties <i>Ramazan Cingi, Bolat Balapanov, Mucteba Uysal, Beyza Fahriye Aygun, Sarsenbek Montayev, Orhan Canpolat</i>	<i>Materials Science</i>	0058
Effect of heat treatment of expanded polystyrene concrete on its compressive strength <i>Tatyana Samoilova, Murat Rakhimov, Galiya Rakhimova, Nurlan Zhangabay</i>	<i>Materials Science</i>	0059
Study of the causes of the collapse of a high-rise chimney under conditions of long-term operation <i>Valentin Mikhailov, Serik Akhmediyev, Daniyar Tokanov,, Nikolai Vatin, Zhmagul Nuguzhinov, Askhat Rakhimov</i>	<i>Construction</i>	0060



Mineral powder based on basalt insulation waste for asphalt concrete

Duman Dyusseminov¹, Rauan Lukpanov¹ Adiya Zhumagulova^{1,*}, Assel Jexembayeva²,
 Beksultan Chugulyov³

¹Department of Technology of Industrial and Civil Engineering, Faculty of Architecture and Construction, L.N. Gumilyov Eurasian National University, 2, Satpayev street, 010008 Astana, Kazakhstan

²Enu-lab research and production center, L.N. Gumilyov Eurasian National University, 2, Satpayev street, 010008 Astana, Kazakhstan

³Testing laboratory, Kazakhstan Road Research Institute, 35, Zhekebatyr street, 010000 Astana, Kazakhstan

*Correspondence: zaaskarovna@gmail.com

Abstract. The article discusses the composition and production technology of mineral powder using waste basalt insulation. This study aims to confirm the hypothesis about the possibility of using basalt waste in the production of mineral powder with technical parameters corresponding to approved standards for the production of asphalt concrete. For definition of qualitative indicators of the received product in comparison with the control sample the researches of the basic indicators of mineral powder according to operating norms are given. Such indicators as grain composition of mineral powder, porosity and density were determined, indicating a more dense structure of the developed composition: the content of particles finer than 0.125 mm – 91.4 %, finer than 0.063 mm – 82.2 % with porosity index 28.1 % and true density 2.49 g/cm³. It was found that the mineral powder from waste basalt mineral slabs has a uniform and balanced grain distribution. At moisture content of samples less than 0.1 % by weight the bitumen capacity index of the tested mineral powder sample in comparison with the control sample showed better value by 2 g, at the same time the degree of swelling of samples from the mixture of powder and bitumen showed better result by 0.1 %. The obtained results indicate that the mineral powder on the basis of waste is able to hold bitumen well on its surface, which contributes to the improvement of adhesion between bitumen and mineral particles. The lower degree of swelling characterizes the increased water resistance and frost resistance of asphalt concrete with the use of this mineral powder. Considering that basalt mineral slabs are waste, their use in the production of mineral powder for asphalt concrete fits into the concept of sustainable construction and can contribute to waste reduction and environmental sustainability of the construction process.

Keywords: mineral powder, waste utilization, resource conservation, property testing, asphalt concrete.

1. Introduction

According to statistical studies on waste disposal by industrial enterprises, about 13000 tons of waste of basalt fiber-based thermal insulation materials and 4350 tons of waste of basalt fiber and materials based on it are generated annually in Kazakhstan [1]. Despite the fact that mineral wool waste accounts for only a small share of total construction waste by mass, it requires large capacities for transportation and disposal due to its low bulk density, and its utilization remains low compared to other types of waste. A study on the utilization of direct waste basalt rock wool produced during the manufacturing process is more suitable for subsequent use due to their high degree of purity than the products after processing [2]. Due to their high content of chemically inert compounds such as silicon dioxide, calcium oxide and aluminum oxide that improve fire retardant properties, mineral wool wastes can be used as fillers in composite materials for construction [3]. In addition, given their potential to absorb petroleum products, mineral wool waste can also be used as an absorbent. We suggest the possibility of solving the problem of environmental protection in the utilization of basalt

board production wastes by processing them into mineral powder. The purpose of the study is to determine the compliance of the technical properties of mineral powder of the proposed composition with the regulatory requirements for mineral powders for asphalt concrete. The objective of the study is to develop a composition of mineral powder from industrial waste for the production of asphalt concrete with technical indicators that meet the approved standards.

In the pursuit of sustainable and green construction, the integration of recycled and waste materials has become the centerpiece of innovation [4–7]. One such pioneering development is the use of waste-derived mineral powder in the production of asphalt concrete. This revolutionary approach not only solves the environmental problems associated with waste management, but also improves the performance and sustainability of asphalt concrete, making it a win-win for both the construction industry and the environment.

Mineral powder from waste materials such as industrial by-products and mining waste provides a valuable alternative to traditional asphalt additives [8–10]. These include materials such as fly ash, slag and other mineral-rich wastes that can be finely ground to produce a high-quality powder suitable for asphalt concrete production. By recycling these materials, the construction industry contributes to reducing the environmental burden associated with waste disposal [11–13].

The inclusion of waste mineral powder significantly improves the performance of asphalt concrete. These waste fillers improve the cohesion and adhesion properties of the asphalt binder, resulting in a more stable and durable pavement structure. The unique composition of the mineral powders can help improve resistance to rutting, cracking and moisture, resulting in longer asphalt pavement life. The technology of mineral powder production implies obtaining an effective additive in asphalt concrete pavement, and is also considered as a way of utilization of basalt mineral insulators production waste, solving the problems of production waste. The composition presented in Table 1 was determined to obtain mineral powder based on basalt insulation waste [14].

Table 1 – Composition of mineral powder based on basalt insulation waste per 0.5 m³ [14]

Type of material	Waste mineral insulation (wool), kg	Water, liters	NaOH, kg	Fuzz, kg	H ₂ SO ₄ , kg
Mineral powder based on waste from basalt insulation materials production	1000	1000	15	30	200

In the production of mineral powder, it is necessary to soak mineral insulation waste with water, temperature not lower than 18 °C. The hydrophobizer is prepared separately: the fuzz is combined with NaOH alkali, the temperature of combination is not lower than 22 °C, and is passed through the RPA (rotary pulsation apparatus), forming a water-soluble emulsion. After the obtained mixture is combined with H₂SO₄ acid and mixed thoroughly, then the obtained mixture is placed in a drying chamber and then in a grinding mill. The obtained powder is sieved and packed.

Figure 1 presents technological scheme of mineral powder production for asphalt concrete.

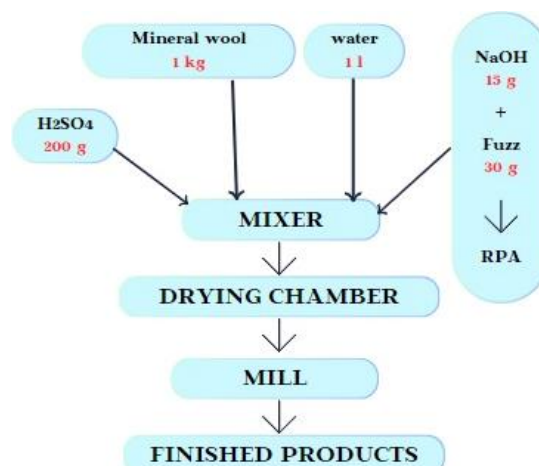


Figure 1 – Scheme for production of mineral powder for asphalt concrete [14]

2. Methods

Studies of the obtained mineral powder on the basis of wastes were carried out in accordance with the current regulations. Mineral powder for asphalt concrete of Temirtau deposit was taken as a control sample. The tests were conducted at the road specialized laboratory of the National Center for the Quality of Road Assets.

2.1 Determination of grain composition

The results of the study of the grain composition of the selected mineral powders will allow an objective assessment of the quality of the structure of the materials [15]. During the test, selected dried samples of mineral powders are poured with a small amount of water and rubbed for up to 2 minutes. The essence of the experiment is the distribution and separation of grains of mineral powder samples by sieving through sieves and determining the residues on each sieve (Figure 2).



Figure 2 – Washing mineral powder through a 0.063 mm sieve

Density and porosity studies were also conducted on the samples to further characterize the mineral powders according to the approved standards [16].

2.2 Determination of moisture content

Laboratory determination of mineral powder moisture content was carried out according to the norms of the national standard [17]. Determining the moisture content of mineral powder is an important quality control step, as moisture content affects its physical and mechanical properties and interaction with bitumen. Moisture is determined by drying the sample to a constant mass.

The essence of the method is to determine the moisture content in the powder (Figure 3).



Figure 3 – Determination of sample weight after drying

A sample of mineral powder with a mass of about 100 g is taken. The exact mass is recorded before drying. The mineral powder sample is dried in a desiccator at 105-110 °C to a constant mass. After drying, the sample is placed in a desiccator to cool to room temperature. The mass of the dried sample is determined. The moisture content of the mineral powder is calculated as the ratio of the mass loss during drying to the initial mass and expressed as a percentage.

2.3 Determination of swelling of mineral powder samples with bitumen

The swelling of mineral powder samples with bitumen was determined to evaluate the interaction between mineral powder and bitumen in asphalt concrete. This parameter is important to prevent undesirable phenomena such as bitumen separation from the mineral aggregate.

The essence of the method is to determine the volume increment of samples with water saturation from 4 % to 5 % by volume from the mixture of powder with bitumen after saturation with water under vacuum conditions and subsequent incubation in hot water (Figure 4).



Figure 4 – Determination of swelling of the mixture with bitumen

The results of each test are evaluated to the first decimal place. The maximum permissible deviation between parallel measurements shall not exceed 0.2 %.

2.4 Determination of bitumen capacity

Tests were also conducted to determine the bituminous capacity of mineral powders to characterize their interaction with bitumen (Figure 5) in accordance with the approved methodology [18-19]. The bitumen capacity of mineral powder is determined to estimate the amount of bitumen required to completely envelop the powder particles.

Mineral powder weighing about 100 grams is dried to a constant mass at 105-110 °C. The cooled powder is placed in an desiccator to prevent absorption of moisture from the air. The bitumen is heated in a thermostat to a temperature of 160 °C. A small amount of the heated bitumen is added to the mineral powder and the mixture is thoroughly mixed until the bitumen is evenly distributed on the surface of the powder particles. The addition of bitumen is continued in batches until all the powder particles are completely covered with bitumen and the mixture has a homogeneous consistency. Bitumen capacity is defined as the ratio of the mass of added bitumen to the mass of mineral powder and is expressed as a percentage. To increase the reliability of the results, the test is repeated three times.



Figure 5 – Determination of bitumen capacity

3. Results and Discussion

This study examined the use of mineral powder obtained from waste basalt mineral slabs in the production of asphalt concrete. Our research focused on studying the effect of mineral filler on asphalt concrete properties: adhesion to bitumen, grain composition, environmental resistance and other important characteristics. Statistical methods of data processing were used to ensure the reliability of the results. The main results and conclusions obtained during the study are presented below.

3.1 Grain composition study

Let us consider the results of the study of grain composition of mineral powder obtained from waste basalt mineral slabs and its influence on the properties of asphalt concrete. The conducted analyses provide an in-depth look at the structure and quality of mineral filler in the context of its application in road pavement construction (Table 2).

Table 2 – Grain composition of studied mineral powders

Type of sample	Grain composition according to GOST, %, not less than			Porosity according to GOST, %, no more than	True density according to GOST, g/cm ³ not standardized
	finer than 2.0 mm	finer than 0.125 mm	finer than 0.063 mm	35	
Control sample	100.0	94.2	78.1	29.0	2.45
Mineral powder based on waste from basalt insulation materials production	100.0	91.4	82.2	28.1	2.49

The obtained results showed a denser structure of mineral powder based on waste mineral insulation boards compared to the control sample, with a minimum content of dusty particles affecting the quality of asphalt concrete. The grain composition study showed that the mineral powder from basalt mineral board waste has a uniform and well-balanced grain distribution. This ensures stability and homogeneity of the internal structure of asphalt concrete.

3.2 Resistant to moisture and chemical influences

The test results showed that the mineral powder based on mineral board production waste has a higher capacity compared to the control sample due to the greater adhesion of bitumen to the surface of mineral particles. Table 3 shows the obtained values of the test results.

Table 3 – Test indicators of interaction with bitumen of mineral powder samples

Type of sample	Swelling of samples from the mixture of powder and bitumen according to GOST, % by volume, not more than	Bitumen capacity index according to GOST, g, not more than	Humidity according to GOST, % by weight, not more than
	2.5	65	1.0
Control sample	2.1	54	less than 0.1
Mineral powder based on waste from basalt insulation materials production	2.0	52	less than 0.1

The obtained value of bituminous capacity of mineral powder based on waste means that to cover a unit mass of mineral powder to the state of complete envelopment of particles it needs less bitumen, compared to the control sample. The high bitumen capacity means that the waste-based mineral powder is able to retain bitumen well on its surface, which helps to improve the bond between the bitumen and the mineral particles. This is important for the strength and durability of asphalt concrete. Knowing bitumen capacity helps to optimize the amount of bitumen in the mix, which helps to save material and improve the technological and performance characteristics of the asphalt concrete.

The degree of swelling of mineral powder characterizes its ability to absorb moisture and increase in volume when in contact with water. This indicator of the sample of mineral powder on the basis of waste is lower than the control one by 0.1%, which characterizes a higher water resistance of mineral powder. The high degree of swelling of mineral powder can increase porosity and reduce the frost resistance of asphalt concrete, which adversely affects the durability of the road surface.

The bituminous capacity index and the degree of swelling of mineral powder are important characteristics [20] that determine the quality and performance of asphalt concrete.

3.3 Environmental feasibility

The use of waste basalt mineral slabs in the production of mineral powder for asphalt concrete will not only improve the technical characteristics of the material, but also make a significant contribution to reducing waste and improving the environmental sustainability of the construction industry. In general, the results of our research emphasize the promising use of mineral powder from basalt mineral slab waste to improve the performance of asphalt concrete, as well as its positive impact on the environmental sustainability of the construction industry.

4. Conclusion

Advantages of using mineral powder from mineral insulation waste in asphalt concrete:

- increased stability and durability;
- the introduction of mineral powder derived from mineral insulation waste strengthens the asphalt mixture, improving its stability and overall durability;
- the unique composition of these mineral powders can improve critical asphalt properties, including resistance to rutting, cracking and moisture.

Processing of construction waste into mineral powder and its use in asphalt pavement is effective from the point of view of environmental protection and resource saving. Our proposed technology of mineral powder production on the basis of recycling of basalt insulators production wastes will allow to obtain high-quality road asphalt concrete with maximum Kazakhstani content and quality indicators in accordance with the standard norms.

The proposed technology of obtaining mineral powder on the basis of recycling of basalt insulation waste as a filler for asphalt concrete is considered for the first time and involves the production of material for road surfaces with an effective bond “binder-mineral filler” to stabilize the main qualitative indicators of asphalt concrete under the influence of temperatures.

Acknowledgement

This research was funded by the Committee of Science of the Ministry of Science and Higher Education of the Republic of Kazakhstan (Grant No. BR21882278 «Establishment of a construction and technical engineering centre to provide a full cycle of accredited services to the construction, road-building sector of the Republic of Kazakhstan»).

The authors would like to express their gratitude to the research and production center «ENU-lab» in conducting laboratory tests of foam concrete.

References

1. Programma proizvodstvennogo ekologicheskogo kontrolya dlya obektov I kategorii. Zavod teploizolyacionnyh materialov po adresu: Respublika Kazahstan, Almatinskaya oblast, Talgarskiy rajon, Industrialnaya zona “Kajrat”. — Almaty: TechnoNICOL Central Asia, 2022. — 50 p.
2. Mineral wool waste in Europe: a review of mineral wool waste quantity, quality, and current recycling methods / O. Väntsi, T. Kärki // *Journal of Material Cycles and Waste Management*. — 2014. — Vol. 16, No. 1. — P. 62–72. <https://doi.org/10.1007/s10163-013-0170-5>
3. Characterization of mineral wool waste chemical composition, organic resin content and fiber dimensions: Aspects for valorization / J. Yliniemi, R. Ramaswamy, T. Luukkonen, O. Laitinen, Á.N. de Sousa, M. Huuhtanen, M. Illikainen // *Waste Management*. — 2021. — Vol. 131. — P. 323–330. <https://doi.org/10.1016/j.wasman.2021.06.022>
4. What we learn is what we earn from sustainable and circular construction / Shashi, P. Centobelli, R. Cerchione, M. Ertz, E. Oropallo // *Journal of Cleaner Production*. — 2023. — Vol. 382. — P. 135183. <https://doi.org/10.1016/j.jclepro.2022.135183>
5. A Comprehensive Overview of the Utilization of Recycled Waste Materials and Technologies in Asphalt Pavements: Towards Environmental and Sustainable Low-Carbon Roads / N.S.A. Yaro, M.H. Sutanto, L. Baloo, N.Z. Habib, A. Usman, A.K. Yousafzai, A. Ahmad, A.H. Birniwa, A.H. Jagaba, A. Noor // *Processes*. — 2023. — Vol. 11, No. 7. — P. 2095. <https://doi.org/10.3390/pr11072095>
6. On The Path towards Sustainable Construction—The Case of the United Arab Emirates: A Review / S.M. Saradara, M.M.A. Khalfan, A. Rauf, R. Qureshi // *Sustainability*. — 2023. — Vol. 15, No. 19. — P. 14652. <https://doi.org/10.3390/su151914652>
7. Circular, Local, Open: A Recipe for Sustainable Building Construction / A. Kouvara, C. Priovolou, D. Ott, P. Scherer, V.H. van Zyl-Bulitta // *Buildings*. — 2023. — Vol. 13, No. 10. — P. 2493. <https://doi.org/10.3390/buildings13102493>
8. Investigating the properties of asphalt concrete containing recycled brick powder as filler / H. Taherkhani, R. Bayat // *European Journal of Environmental and Civil Engineering*. — 2022. — Vol. 26, No 8. — P. 3583–3593. <https://doi.org/10.1080/19648189.2020.1806932>
9. Utilization of Construction Waste Recycled Powder as Filler in Asphalt Concrete / Z. Guo, Z. Chen // *Materials*. — 2022. — Vol. 15, No. 16. — P. 5742. <https://doi.org/10.3390/ma15165742>
10. Mechanical Characterization of Industrial Waste Materials as Mineral Fillers in Asphalt Mixes: Integrated Experimental and Machine Learning Analysis / N. Tiwari, N. Baldo, N. Satyam, M. Miani // *Sustainability*. — 2022. — Vol. 14, No. 10. — P. 5946. <https://doi.org/10.3390/su14105946>
11. Life cycle assessment of roadworks in United Arab Emirates: Recycled construction waste, reclaimed asphalt pavement, warm-mix asphalt and blast furnace slag use against traditional approach / U. Hasan, A. Whyte, H. Al Jassmi // *Journal of Cleaner Production*. — 2020. — Vol. 257. — P. 120531. <https://doi.org/10.1016/j.jclepro.2020.120531>
12. Construction and demolition waste management contributing factors coupled with reduce, reuse, and recycle strategies for effective waste management: A review / K. Kabirifar, M. Mojtahedi, C. Wang, V.W.Y. Tam // *Journal of Cleaner Production*. — 2020. — Vol. 263. — P. 121265. <https://doi.org/10.1016/j.jclepro.2020.121265>
13. Critical evaluation of construction and demolition waste and associated environmental impacts: A scientometric analysis / K. Chen, J. Wang, B. Yu, H. Wu, J. Zhang // *Journal of Cleaner Production*. — 2021. — Vol. 287. — P. 125071. <https://doi.org/10.1016/j.jclepro.2020.125071>
14. Development of the composition of mineral powder for asphalt concrete: copyright 42252 / Zhumagulova A., Dzheksembaeva A., Dyusembinov D., Lukpanov R., Shakhmov Zh.; publ. 2024.

15. GOST 32719-2014. Automobile roads of general use. Mineral powder. Method of determination of the grain. — 2014.
16. GOST 32764-2014. Automobile roads of general use. Mineral powder. Method for determination of medium density and porosity. — 2014.
17. ST RK 1221-2003. Mineral powder for asphalt-concrete mixtures. Testing methods. — 2003.
18. GOST 32707-2014. Automobile roads of general use. Mineral powder. Method for determination of swelling samples from a mixture of powder with bitumen. — 2014.
19. GOST 32766-2014. Automobile roads of general use. Mineral powder. Method of definition of the indicator characterizes the quantity of oil. — 2014.
20. GOST 16557-2005. Mineral powders for asphaltic concrete and organomineral mixtures. Specifications — 2005.

Information about authors:

Duman Dyusembinov – Candidate of Technical Sciences, Associate Professor, Department of Technology of Industrial and Civil Engineering, Faculty of Architecture and Construction, L.N. Gumilyov Eurasian National University, 2, Satpayev street, 010008, Astana, Kazakhstan, dusembinov@mail.ru

Rauan Lukpanov – PhD, Professor, Department of Technology of Industrial and Civil Engineering, Faculty of Architecture and Construction, L.N. Gumilyov Eurasian National University, 2, Satpayev street, 010008, Astana, Kazakhstan, rauan_82@mail.ru

Adiya Zhumagulova – Candidate of Technical Sciences, Associate Professor, Department of Technology of Industrial and Civil Engineering, Faculty of Architecture and Construction, L.N. Gumilyov Eurasian National University, 2, Satpayev street, 010008, Astana, Kazakhstan, zaaskarovna@gmail.com

Assel Jexembayeva – PhD, Director, Innovation Development Department, L.N. Gumilyov Eurasian National University, 2, Satpayev street, 010008, Astana, Kazakhstan, dzheksembayeva_ae@mail.ru

Beksultan Chugulyov – Engineer, Testing laboratory, Kazakhstan Road Research Institute, 35, Zhekebatyr street, 010000 Astana, Kazakhstan, beksultan_d@mail.ru

Author Contributions:

Duman Dyusembinov – concept, methodology, analysis.

Rauan Lukpanov – analysis, interpretation, drafting.

Adiya Zhumagulova – data collection, visualization, editing.

Assel Jexembayeva – resources, funding acquisition.

Beksultan Chugulyov – testing.

Conflict of Interest: The authors declare no conflict of interest.

Use of Artificial Intelligence (AI): The authors declare that AI was not used.

Received: 27.05.2024

Revised: 12.06.2024

Accepted: 13.06.2024

Published: 13.06.2024



Copyright: © 2024 by the authors. Licensee Technobius, LLP, Astana, Republic of Kazakhstan. This article is an open access article distributed under the terms and conditions of the Creative Commons Attribution (CC BY-NC 4.0) license (<https://creativecommons.org/licenses/by-nc/4.0/>).



Experimental study of sound wave propagation patterns

Alisher Imanov¹, Aigul Kozhas², Assel Mukhamejanova¹, Aida Nazarova³,
 Dias Kazhimkanuly^{1,*}

¹Department of Civil Engineering, L.N. Gumilyov Eurasian National University, Astana, Kazakhstan

²Department of Technology of Industrial and Civil Construction, L.N. Gumilyov Eurasian National University, Astana, Kazakhstan

³Department of Physics, Nazarbayev University, Astana, Kazakhstan

*Correspondence: dias27049795@gmail.com

Abstract. The present study compares the behavior of different sound types and their sources concerning distance. Experimental findings demonstrate a consistent reduction in noise levels with increasing distance from the sound origin, aligning with anticipated sound propagation patterns. Median noise level reductions are quantified, showing decreases from 72.7 dB at the source to 54.8 dB at a distance of 3 m. Pulsed sounds exhibit pronounced fluctuations and peaks at close distances, while steady and blended sounds maintain more uniform levels. An exponential model accurately characterizes the noise reduction phenomenon ($R^2 = 0.8664$), underscoring its applicability for construction noise control. These results offer valuable insights into sound propagation dynamics and provide a basis for developing effective noise control strategies.

Keywords: sound waves, sound propagation, noise levels, acoustic engineering, measurement.

1. Introduction

The study of sound wave propagation patterns is important for both basic science and applied fields such as acoustics, structural engineering and ecology [1,2]. Understanding the mechanism of sound wave propagation contributes to improving the quality of sound environments, developing more effective noise insulation materials and technologies, and optimizing the acoustic performance of rooms and open spaces [3–6].

In the modern world, the level of noise pollution is constantly increasing, which negatively affects the health and well-being of people [3,6]. Problems related to excessive noise are becoming more and more relevant in urban and industrial areas, and construction sites [2,4,7]. In this regard, accurate data on the behavior of sound waves in different environments are needed to develop effective noise control methods and improve acoustic comfort in living and working spaces [8].

Despite a significant amount of research in acoustics, there is a lack of data concerning the behavior of sound waves in different environments and conditions. Frequently arising questions are related to the influence of different types of sound sources and distances on noise levels, which requires additional experimental studies and validation of theoretical models [9].

A pulsed sound is a sound that occurs in individual rhythmic bursts or pulses. These bursts can vary in intensity and frequency, creating a characteristic pattern [10,11].

Steady sound, means a constant and unchanging sound without fluctuations or variations in amplitude or frequency, which often come from mechanical or environmental sources [12,13].

A blended sound is a mixture or combination of different sounds occurring simultaneously, resulting in a complex auditory experience [14].

Choosing these types of sounds to experiment with allows us to explore different aspects of auditory perception and cognition. Impulsive sounds allow precise timing and synchronization of events, sustained sounds provide a stable background for comparison, and mixed sounds reflect the complexity of actual auditory experience. These diverse types of sounds allow the experiment to be designed to reflect the variability of auditory stimuli encountered in everyday life.

The purpose of this study is to investigate the propagation patterns of sound waves of various types under controlled conditions. The study aims to obtain quantitative data on the behavior of sound waves and their variation as a function of distance from the sound source.

In order to achieve the set goal, the following tasks should be solved:

- Develop and manufacture experimental racks for equipment placement.
- Prepare and set up measuring devices for fixing the sound level.
- Conduct a series of experiments with different types of sound sources (pulsed, steady and blended).
- Collect and analyze data on sound levels at different distances from a source.
- Draw conclusions about the patterns of sound wave propagation based on the data obtained.

This study will contribute to the knowledge of sound wave propagation mechanisms and the development of effective methods for controlling and managing noise in different environments, including construction sites.

2. Methods

2.1 Preparation of experimental racks

The preparation of experimental racks is a critical step to ensure accurate and consistent data collection. For this experiment, specialized racks were designed (Figure 1) and constructed following a specific layout to meet the requirements of the study. The racks were crafted from wooden material, selected for its durability and ease of manipulation. Each board connection was reinforced using four screws on each side, ensuring structural stability and rigidity. The schematic drawing of the racks provided precise dimensions for each component (Figure 1). These dimensions were meticulously adhered to during the manufacturing process to ensure uniformity across all racks used in the experiments. To minimize the influence of external vibrations, particularly from the ground, the surfaces of the racks were covered with a 10 mm layer of sponge (Figure 2).

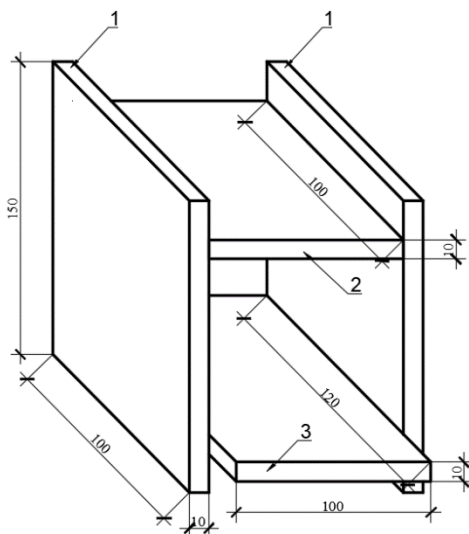


Figure 1 – Schematic drawing of the stand for the experiment. Board dimensions:
 1 – 150x100x10 mm; 2 – 100x100x10 mm;
 3 – 120x100x10 mm

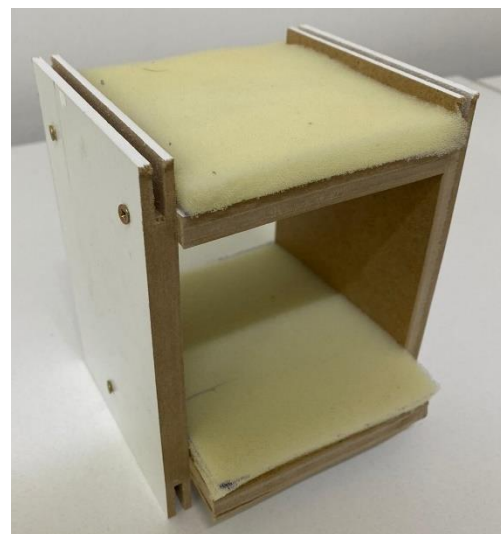


Figure 2 – Experiment stand

This cushioning material was chosen for its effectiveness in dampening vibrations, thereby ensuring that the measurements taken were not affected by extraneous movement or noise. Four identical racks were produced for use in the experiments.

2.2 Placement of racks and equipment

Proper placement of the racks and equipment was essential to maintain the integrity of the experiment. The first rack was strategically positioned directly at the sound source (Figure 3). This placement was crucial for capturing the initial sound intensity and variations at the point of origin. The remaining racks were placed at intervals of one meter from the sound source, forming a linear arrangement. This linear sequence allowed for the systematic measurement of sound intensity at increasing distances from the source, providing a clear gradient of sound propagation.



Figure 3 – Placement of racks

Each rack was equipped with two key pieces of equipment:

1. Video Fixation Devices: The upper part of each rack was designated for mounting video fixation devices (Figure 4). These devices, fixed on phones, were used to visually document the experiment and ensure the precise timing of measurements.

2. Noise Level Meters: The lower part of each rack was designed to hold UT352 (Figure 4) noise level meters. These meters, manufactured by UNI-T, were chosen for their reliability and accuracy. They are certified and listed in the Register of Standard Measuring Instruments of the Republic of Kazakhstan, ensuring compliance with measurement standards.



Figure 4 – Placement of the noise meter on the rack

The careful positioning of these devices was critical for capturing accurate sound levels at each specified distance.

2.3 Conducting the experiment

Three different types of sound sources were used during the experiment:

- Pulsed sound: this involved brief, pulsed sounds designed to simulate sudden noise bursts.
- Steady sound: this type involved a steady, uninterrupted sound, representing a constant noise source.

- Blended sound: This included complex sounds with varying frequencies and time characteristics, simulating more natural and varied noise environments.

For each type of sound source, measurements were taken over a specific time interval of 5 seconds. During this interval, the noise level meters recorded the sound intensity at a high sampling rate, capturing 8 values per second. This high temporal resolution ensured that even small fluctuations in sound intensity were recorded, providing a detailed dataset for analysis. The measurements were taken at four different distances from the sound source: at the source (0 meters); 1 meter from the source; 2 meters from the source; 3 meters from the source. This setup allowed the researchers to observe how sound intensity diminished with distance, a fundamental aspect of sound wave propagation. The data collected from these measurements were then analyzed to identify patterns in sound propagation and to understand how different types of sounds behave over distance.

The overall methodology ensured that the experiment was conducted in a systematic and controlled manner, allowing for the collection of reliable and accurate data on sound wave propagation. The results of this experiment are expected to provide valuable insights into noise control and management.

3. Results and Discussion

The experiment was conducted to measure the Sound Pressure Level (SPL) of pulsed, steady, and blended sound in decibels (dB) at four posts located at different distances from the sound source. Figure 5-7 presents the results of these measurements.

0: a stand that is directly at the sound source; 1: a stand that is 1 meter away from the source; 2: a stand that is 2 meters away from the source; 3: a rack that is 3 meters away from the source.

3.1 Pulsed sound in decibels (dB)

The graph (Figure 5) shows the variation in noise level for each of the 40 measurements:

- 0 m: noise level varies from 59.7 to 73.3 dB;
- 1 m: noise level varies from 43.4 to 66.0 dB;
- 2 m: noise level varies from 40.3 to 65.4 dB;
- 3 m: noise level varies from 39.6 to 59.9 dB.

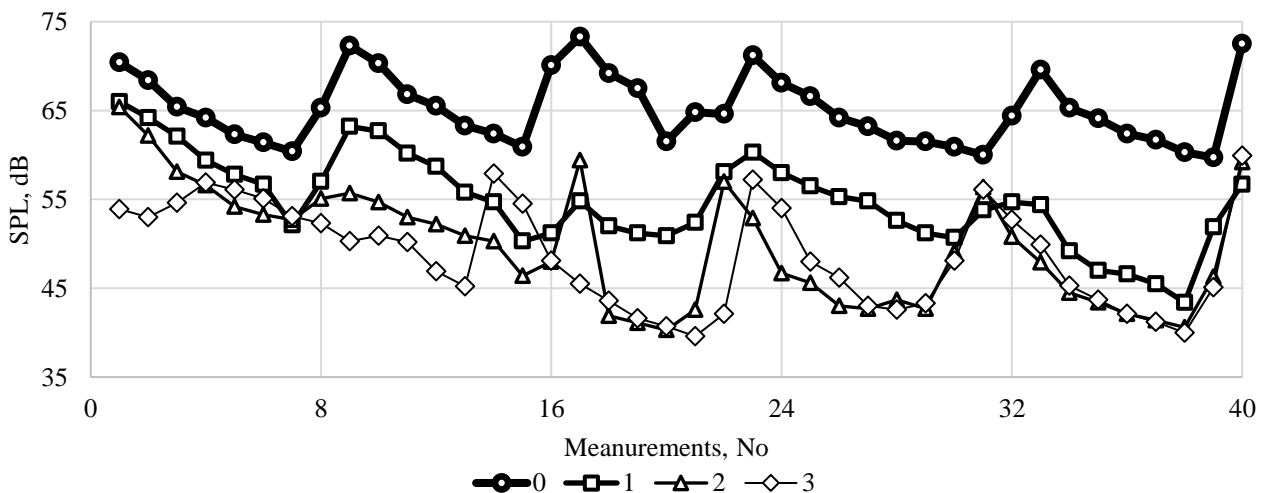


Figure 5 – Pulsed sound

The noise level decreases as the distance from the sound source increases. In all cases, there is a general tendency for the noise level to decrease from the beginning to the end of the measurements. More pronounced fluctuations and peaks in noise level are observed at the post located at the sound source (blue line) compared to the rest of the posts.

3.2 Steady sound in decibels (dB)

The graph (Figure 6) shows the variation in noise level for each of the 40 measurements:

- 0 m: noise level varies from 74.3 to 85.5 dB;
- 1 m: noise level varies from 65.0 to 69.1 dB;
- 2 m: noise level varies from 62.7 to 65.6 dB;
- 3 m: noise level varies from 61.0 to 63.4 dB.

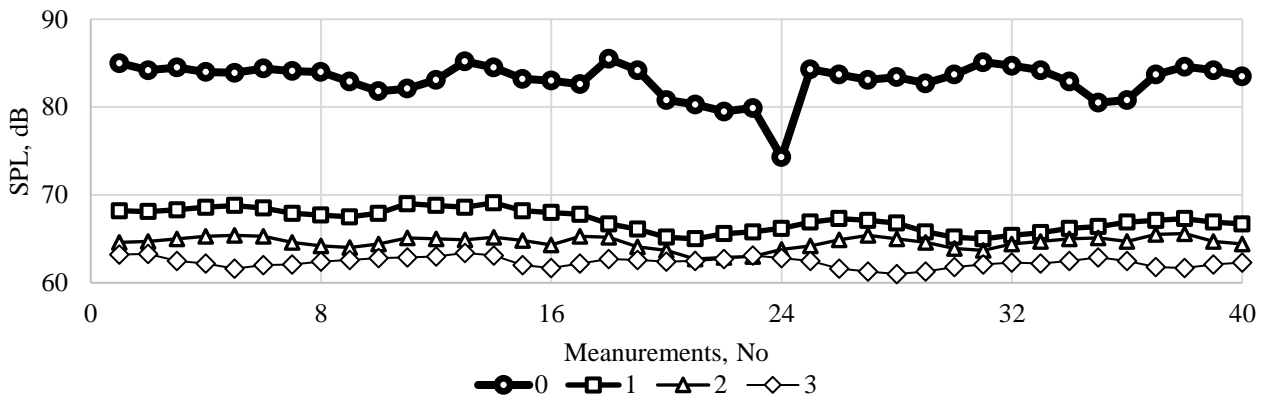


Figure 6 – Steady sound

The noise concentration decreases as the distance from the sound source increases. The rack located directly at the sound source (orange line) shows significant fluctuations in the noise level in the middle of the measurements, while at the other racks the noise level remains almost uniform.

3.3 Blended sound in decibels (dB)

The graph (Figure 7) shows the variation in noise level for each of the 40 measurements:

- 0 m: noise level varies from 74.3 to 85.5 dB;
- 1 m: noise level varies from 65.0 to 69.1 dB;
- 2 m: noise level varies from 62.7 to 65.6 dB;
- 3 m: noise level varies from 61.0 to 63.4 dB.

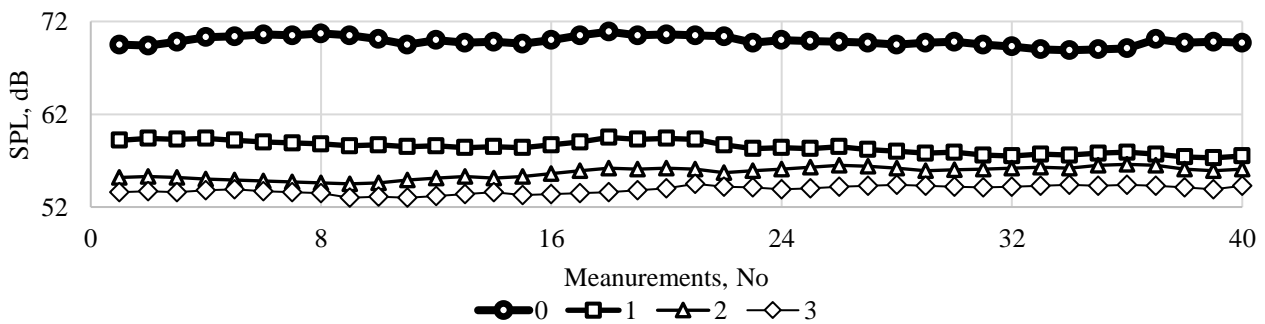


Figure 7 – Blended sound

Noise intensity decreases with increasing distance from the sound source. Nevertheless, the noise level at the measuring stand located directly at the source (orange line) is significantly higher than the values recorded at the other stands. In all cases, the noise level is almost evenly distributed.

The graph (Figure 8) shows a general trend of decreasing sound level with increasing distance from the source, based on median values. The pulsed sound starts at 64.5 dB at 0 meters and decreases to 48.1 dB at 3 meters. The steady sound starts at 83.7 dB at a distance of 0 meters and decreases to 62.4 dB at a distance of 3 meters. The blended sound starts at 69.8 dB at a distance of 0 meters and decreases to 53.9 dB at a distance of 3 meters. The average sound starts at about 70 dB at a distance of 0 meters and decreases to 55 dB at a distance of 3 meters. The exponential trend line follows the average sound points with a strong correlation ($R^2 = 0.8664$).

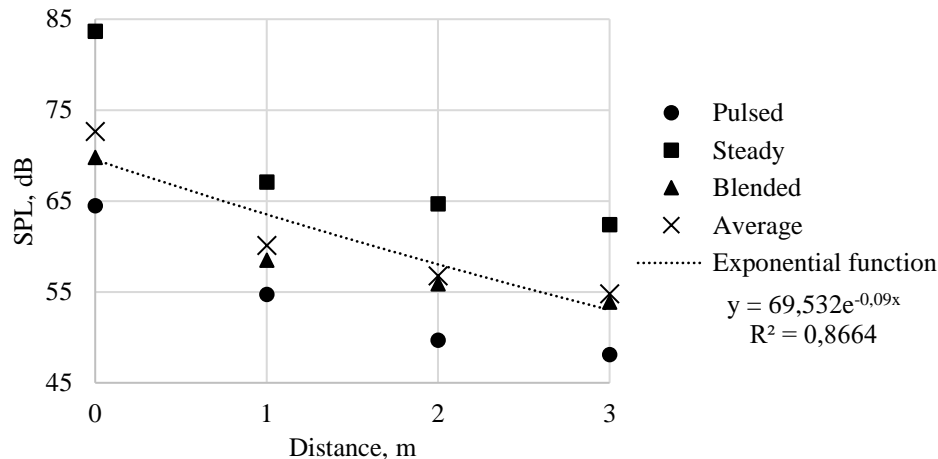


Figure 8 – Analysis of sound propagation

The sound level decreases as the distance from the source increases, which is consistent with the physical behavior of sound propagation in open space [15]. The exponential decay model agrees well with the average sound data, indicating that the decrease in sound level is exponential. The coefficient of determination ($R^2 = 0.8664$) indicates a good fit of the exponential model to the observed data. This analysis provides insight into how sound level decreases with distance, which can be useful in construction noise control.

4. Conclusions

In this paper, different types of sounds and their potential sources were investigated as a function of distance. Experimental results show a clear decrease in noise level with increasing distance from the sound source for pulsed, steady, and blended sounds, which is consistent with the expected physical behavior of sound propagation. Numerical values include a median noise level reduction from 72.7 dB at the source to 54.8 dB at a distance. Pulsed sounds are observed to exhibit greater fluctuations and peaks at close distances, with the median level starting at 70.4 dB and decreasing to 59.9 dB. Steady and blended sounds have more uniform noise levels, with steady sounds decreasing from 66 dB to 56.7 dB and blended sounds decreasing from 65.4 dB to 59.2 dB. The exponential model accurately describes noise reduction with a high coefficient of determination ($R^2 = 0.8664$), which emphasizes its applicability for construction noise control.

Acknowledgments

This research was funded by the Science Committee of the Ministry of Science and Higher Education of the Republic of Kazakhstan (Grant No. AP19674718).

References

1. Fundamentals of Acoustic Wave Generation and Propagation / M.A. Sahin, M. Ali, J. Park, G. Destgeer // Acoustic Technologies in Biology and Medicine. — Hoboken, USA: Wiley, 2023. — P. 1–36. <https://doi.org/10.1002/9783527841325.ch1>

2. Acoustics, Linear / J.E. Greenspon // Encyclopedia of Physical Science and Technology. — Amsterdam, Netherlands: Elsevier, 2003. — P. 129–167. <https://doi.org/10.1016/B0-12-227410-5/00009-0>
3. Recent progress in acoustic materials and noise control strategies – A review / Y. Tao, M. Ren, H. Zhang, T. Peijs // Applied Materials Today. — 2021. — Vol. 24. — P. 101141. <https://doi.org/10.1016/j.apmt.2021.101141>
4. Outdoor Sound Propagation / D. Habault // AcousticsElsevier, 1999. — P. 121–157. <https://doi.org/10.1016/B978-012256190-0/50005-1>
5. Active times for acoustic metamaterials / F. Zangeneh-Nejad, R. Fleury // Reviews in Physics. — 2019. — Vol. 4. — P. 100031. <https://doi.org/10.1016/j.revip.2019.100031>
6. Community Noise, Urbanization, and Global Health: Problems and Solutions / C.M. Salter, R. Ahn, F. Yasin, R. Hines, L. Kornfield, E.C. Salter, T.F. Burke // Innovating for Healthy Urbanization. — Boston, MA: Springer US, 2015. — P. 165–192. https://doi.org/10.1007/978-1-4899-7597-3_8
7. The future of urban sound environments: Impacting mobility trends and insights for noise assessment and mitigation / A. Can, A. L’Hostis, P. Aumond, D. Botteldooren, M.C. Coelho, C. Guarnaccia, J. Kang // Applied Acoustics. — 2020. — Vol. 170. — P. 107518. <https://doi.org/10.1016/j.apacoust.2020.107518>
8. Breaking the limits of acoustic science: A review of acoustic metamaterials / G. Aydın, S.E. San // Materials Science and Engineering: B. — 2024. — Vol. 305. — P. 117384. <https://doi.org/10.1016/j.mseb.2024.117384>
9. Indicators and methods for assessing acoustical preferences and needs of students in educational buildings: A review / A. Hamida, D. Zhang, M.A. Ortiz, P.M. Bluyssen // Applied Acoustics. — 2023. — Vol. 202. — P. 109187. <https://doi.org/10.1016/j.apacoust.2022.109187>
10. Linear propagation of a pulsed sound beam from a plane or focusing source / K.-E. Froysa, J.N. Tjo/tta, S. Tjo/tta // The Journal of the Acoustical Society of America. — 1993. — Vol. 93, No. 1. — P. 80–92. <https://doi.org/10.1121/1.405546>
11. Pulsed Noise Experience Disrupts Complex Sound Representations / M.N. Insanally, B.F. Albanna, S. Bao // Journal of Neurophysiology. — 2010. — Vol. 103, No. 5. — P. 2611–2617. <https://doi.org/10.1152/jn.00872.2009>
12. Acoustic metacages for sound shielding with steady air flow / C. Shen, Y. Xie, J. Li, S.A. Cummer, Y. Jing // Journal of Applied Physics. — 2018. — Vol. 123, No. 12. — P. 124501. <https://doi.org/10.1063/1.5009441>
13. Steady Beat Sound Facilitates both Coordinated Group Walking and Inter-Subject Neural Synchrony / S. Ikeda, T. Nozawa, R. Yokoyama, A. Miyazaki, Y. Sasaki, K. Sakaki, R. Kawashima // Frontiers in Human Neuroscience. — 2017. — Vol. 11. — P. 147. <https://doi.org/10.3389/fnhum.2017.00147>
14. Blended noise suppression using a hybrid median filter, normal moveout and complex curvelet transform approach / L. Dong, C. Wang, M. Zhang, D. Wang, X. Liang // Studia Geophysica et Geodaetica. — 2020. — Vol. 64, No. 2. — P. 241–254. <https://doi.org/10.1007/s11200-020-0269-9>
15. Fundamentals of Wave Propagation / M. Möser // Engineering Acoustics. — Berlin, Heidelberg: Springer Berlin Heidelberg, 2004. — P. 13–41. https://doi.org/10.1007/978-3-662-05391-1_2

Information about authors:

Alisher Imanov – PhD Student, Department of Civil Engineering, L.N. Gumilyov Eurasian National University, Astana, Kazakhstan, glad.alisher@gmail.com

Aigul Kozhas – Candidate of Technical Sciences, Senior Lecturer, Department of Technology of Industrial and Civil Construction, L.N. Gumilyov Eurasian National University, Astana, Kazakhstan, kozhas@bk.ru

Assel Mukhamejanova – PhD, Senior Lecturer, Department of Civil Engineering, L.N. Gumilyov Eurasian National University, Astana, Kazakhstan, assel.84@list.ru

Aida Nazarova – PhD, Laboratory Instructor, Department of Physics, Nazarbayev University, Astana, Kazakhstan, aida_m@list.ru

Dias Kazhimkanuly – PhD Student, Department of Civil Engineering, L.N. Gumilyov Eurasian National University, Astana, Kazakhstan, dias27049795@gmail.com

Author Contributions:

Alisher Imanov – concept, methodology.

Aigul Kozhas – resources, analysis.

Assel Mukhamejanova – visualization, interpretation.

Aida Nazarova – drafting, editing, funding acquisition.

Dias Kazhimkanuly – data collection, testing, modeling.

Conflict of Interest: The authors declare no conflict of interest.

Use of Artificial Intelligence (AI): The authors declare that AI was not used.

Received: 27.05.2024

Revised: 11.06.2024

Accepted: 13.06.2024

Published: 14.06.2024



Copyright: @ 2024 by the authors. Licensee Technobius, LLP, Astana, Republic of Kazakhstan. This article is an open access article distributed under the terms and conditions of the Creative Commons Attribution (CC BY-NC 4.0) license (<https://creativecommons.org/licenses/by-nc/4.0/>).



Alkali-activated composites with synthetic fibers and recycled aggregates: a study of mechanical properties

Ramazan Cingi¹, Bolat Balapanov^{2,*}, Mucteba Uysal³, Beyza Fahriye Aygun¹,
 Sarsenbek Montayev⁴, Orhan Canpolat³

¹Department of Civil Engineering, Istanbul University-Cerrahpasa, Üniversite Yolu No:2, 34320 Avcılar, Istanbul, Turkey

²Department of Architecture and Construction, Korkyt Ata Kyzylorda University, Aiteke bi 29 A, Kyzylorda, Kazakhstan

³Department of Civil Engineering, Yıldız Technical University, Barbaros Bulvarı 34349, Yıldız, Istanbul, Turkey

⁴Industrial Technological Institute, Zhangir Khan West-Kazakhstan Agrarian and Technical University, 51 Zhangir Khan Street, Uralsk, Kazakhstan

*Correspondence: balapanov.sci@gmail.com

Abstract. This study examines the potential for enhancing alkali-activated composites (AACs) through the incorporation of a blend of meta-zeolite (MZ) and slag, reinforced with synthetic fibers and incorporating aluminum sludge (AS) and recycled concrete aggregate. AACs were activated with sodium hydroxide (NaOH) and sodium silicate (Na₂SiO₃) in varying ratios and molarities (8M to 14M). The optimal mix, comprising 50% MZ and 50% S at 12M NaOH with 30% AS, exhibited notable enhancements in mechanical properties. Specifically, the addition of 0.5% basalt fibers resulted in a 7.26% increase in compressive strength and a 24.15% enhancement in flexural strength. These findings underscore the potential of MZ-S-based AACs, enhanced with aluminum sludge and basalt fiber, to develop advanced, sustainable construction materials. The study underscores the significance of optimizing material ratios and reinforcement strategies to achieve superior performance, thereby contributing to the development of environmentally friendly building solutions that align with contemporary standards.

Keywords: alkali-activated composites, metazeolite, synthetic fibers, environmental standards, recycled concrete aggregate.

1. Introduction

The demand for sustainable development in civil engineering has increased significantly in recent years, as the need for eco-friendly and cost-effective construction materials has become more pressing. Conventional construction methods rely heavily on Portland cement (PC), a material with a significant environmental footprint, contributing approximately 7% to global CO₂ emissions. As the industry seeks alternatives, alkali-activated composites (AACs) have emerged as a promising solution, offering reduced CO₂ emissions and lower energy consumption. This investigation focuses on the usage of metazeolite (MZ) and slag (S) in AACs, enhanced with AS and recycled concrete aggregate (RCA), to create high-performance, sustainable building materials. The phenomenon of urbanization has led to an increase in construction and demolition activities, which has resulted in a considerable amount of waste being generated. In regions prone to earthquakes, such as Turkey, urban transformation projects are anticipated to produce approximately 2 billion tons of construction waste over the next two decades. This presents a unique opportunity to recycle this waste into valuable construction materials, addressing both environmental and economic concerns. Utilisation of RCAs in AACs not only addresses the issue of disposal but also reduces the demand for virgin raw materials, thereby aligning with the principles of sustainable development [1, 2].

Research into AACs has revealed that the incorporation of various fibers can significantly enhance their mechanical properties. Synthetic fibers, such as polyethylene (PEF), polyamide (PAF), and basalt fibers (BF), have demonstrated particular promise. These fibers enhance the structural integrity of AACs by improving tensile and flexural strengths, reducing crack propagation, and improving overall durability. Sahin et al. [3] investigated the impact of different BF ratios in MK-based AACs with various aggregate types. Although mechanical strengths remained acceptable, AACs with recycled aggregate displayed slightly lower properties.

Natural zeolites, with their unique chemical structures, play a crucial role in the geopolymerization process of AACs. The calcination of these materials at specific temperatures enhances their reactivity, allowing for the creation of robust and durable composites. Zheng et al. [4] compared the frost resistance of concrete using calcined zeolite, showing improved porosity and pore structure with curing age. Similarly, Florez et al. [5] investigated the calcination-pre-grinding processes of zeolite, revealing enhanced pozzolanic properties. Nikolov et al. [6] utilized calcined natural zeolite and clinoptilolite as AAC precursors, achieving high compressive strength with potassium silicate activation. Further studies by Ozen and Alam [7] emphasized the significance of activator ratios in the geopolymerization of zeolite-based AACs. Aygörmez [8] analyzed the high-temperature effects of MK-S-based AACs reinforced with BF, demonstrating stability even after exposure to 750 °C. The integration of AS into AACs presents a novel approach to waste management and material enhancement. AS, a by-product of alumina production, is typically considered a disposal challenge due to its fine particle size and potential environmental impact. Nevertheless, its incorporation into AACs can facilitate setting and enhance compressive strength, rendering it a valuable component in sustainable construction materials. This study examines the synergistic effects of AS and fiber reinforcement in AACs, providing a comprehensive analysis of their mechanical properties and durability. The combination of zeolite and fibers enhances compressive strength and abrasion resistance. Investigations on ultra-high-performance AACs (UHPAACs) with PPF and SF have revealed enhanced mechanical properties, particularly with PPF in SF samples. Non-destructive testing, such as UPV, has been used to assess SF-reinforced concrete with recycled nylon granules and zeolite, demonstrating improved properties [9-29].

Steel fibers (SF) and BFs have been identified as effective in enhancing the workability and strength of alkali-activated materials or AACs. The combined use of SF and BF results in a synergistic improvement in hardening, a reduction in stress concentration, and a limitation of crack formation. While SF enhances the internal structure and properties, BF contributes to forming a well-defined interfacial region, improving water absorption and porosity. The incorporation of these fibers into customizable composite materials allows for the achievement of optimal performance at a nominal cost, thereby enhancing environmental friendliness. Moreover, integrating natural fiber reinforcement into traditional composites represents a viable and sustainable approach, both environmentally and economically. Researchers have utilized various fibers to improve the properties of AACs. Choi et al. [30] observed that incorporating PEF-PVAF reinforcement in S-based AACs enhanced tensile capacity and healing performance compared to PEF alone. Wang et al. investigated the effects of PVA fiber and nano-silica on MK-S-based AACs, observing significant strength and durability improvements with optimal PVAF and NS blends. Shaikh [31] examined PPF as a reinforcement fiber, concluding that PPF composites exhibited superior mechanical properties with an optimum fiber content of 0-1% by volume due to reduced workability.

This study underscores the eco-technological advantages of sustainable AACs in construction. The global construction industry contributes significantly to environmental pollution and greenhouse gas emissions, primarily due to extensive PC usage and solid waste buildup. Developed countries have initiated regulatory measures to control PC emissions and promote waste concrete recycling. In Turkey, recycling is paramount, particularly in light of the environmental impact of debris from earthquakes and urban transformations. This research underscores the significance of sustainable AAC production, illustrating such materials' ecological benefits and technological adaptability in the context of evolving environmental concerns in the construction industry.

2. Methods

2.1 Raw materials and their properties

This study employed various materials to create alkali-activated composites (AACs). Slag (S), obtained from the Bolu Cement Industry, was used due to its high specific gravity (SG) of 2.9 and an impressive 98.6% pass rate through a 45-micron sieve. Mec Energy supplied the zeolite with a specific gravity of 2.17 and a significant surface area of 9660 cm²/g. The zeolite underwent calcination at 900 °C to enhance its reactivity. Aluminum sludge (AS) was procured from Eti Aluminum AS, dried at 105 °C, and milled to a 90 µm particle size. Recycled concrete aggregate (RCA), provided by a local recycling company, featured an SG of 2.05 and was sieved through a 2 mm sieve to obtain fine aggregates. The chemical activators used included NaOH with a purity exceeding 99% and Na₂SiO₃ containing 27.2% SiO₂, 8.2% Na₂O, with a pH range of 11-12.4. Table 1 presents the chemical compositions of these binder materials.

Table 1 – Chemical Composition of Binder Materials

Component	Slag (%)	Metazeolite (MZ) (%)	Red Mud (RM) (%)	RCA (%)
SiO ₂	40.55	76.90	16.20	62.56
Al ₂ O ₃	12.83	13.50	22.90	12.52
Fe ₂ O ₃	1.10	1.40	34.50	5.82
TiO ₂	0.75	0.10	-	0.75
CaO	35.58	2.00	1.80	12.01
MgO	5.87	1.10	-	1.83
K ₂ O	0.68	3.50	-	1.30
Na ₂ O	0.79	0.30	8.70	2.69
LOI	0.03	1.10	-	-
MnO	-	0.10	-	0.12

2.2 Mix design

AACs were formulated with a sand-to-binder ratio of 2.5 and an activator-to-binder ratio of 0.95. The weight ratio of Na₂SiO₃ to NaOH was maintained at 2:1, in line with both literature guidelines and preliminary laboratory tests. The initial phase involved creating 16 different AAC mixes, categorized into four series based on varying binder compositions: 100% MZ, 75% MZ + 25% S, 50% MZ + 50% S, and 75% S + 25% MZ. Each series was tested with four NaOH molarities: 8M, 10M, 12M, and 14M. The mix that demonstrated the highest strength in this phase underwent further testing with the addition of 10%, 20%, and 30% AS to assess its impact on compressive strength, flexural strength (at 7 and 28 days) and water absorption ratios (at 28 days). In the final phase, based on the optimal mix of MZ-S and AS, the influence of synthetic fibers—BF, PEF, and PAF at various percentages (0.5%, 1%, 1.5%, and 2%) was analyzed for their mechanical properties (Table 2).

Table 2 – Mixture Contents and Quantities

Mixing Code	MZ (g)	AS (g)	S (g)	RCA (g)	Na ₂ SiO ₃ (g)	NaOH (g)	PEF (g)	PAF (g)	BF (g)
100MZ	450	-	-	1125	142.5	285	-	-	-
75MZ+25S	337.5	-	112.5	1125	142.5	285	-	-	-
50MZ+50S (C)	225	-	225	1125	142.5	285	-	-	-
75S+25MZ	112.5	-	337.5	1125	142.5	285	-	-	-
50MZ+50S+10AS	225	112.5	225	1012.5	142.5	285	-	-	-

Mixing Code	MZ (g)	AS (g)	S (g)	RCA (g)	Na ₂ SiO ₃ (g)	NaOH (g)	PEF (g)	PAF (g)	BF (g)
50MZ+50S+20AS	225	225	225	900	142.5	285	-	-	-
50MZ+50S+30AS	225	337.5	225	787.5	142.5	285	-	-	-
C+30AS+0.5PEF	225	337.5	225	783.22	142.5	285	4.28	-	-
C+30AS+1PEF	225	337.5	225	774.67	142.5	285	8.55	-	-
C+30AS+1.5PEF	225	337.5	225	761.85	142.5	285	12.82	-	-
C+30AS+2PEF	225	337.5	225	744.75	142.5	285	17.1	-	-
C+30AS+0.5PAF	225	337.5	225	784.09	142.5	285	-	3.41	-
C+30AS+1PAF	225	337.5	225	781.22	142.5	285	-	6.82	-
C+30AS+1.5PAF	225	337.5	225	764.44	142.5	285	-	10.23	-
C+30AS+2PAF	225	337.5	225	748.2	142.5	285	-	13.65	-
C+30AS+0.5BF	225	337.5	225	734.63	142.5	285	-	-	10.12
C+30AS+1BF	225	337.5	225	763.84	142.5	285	-	-	20.25
C+30AS+1.5BF	225	337.5	225	750.85	142.5	285	-	-	30.37
C+30AS+2BF	225	337.5	225	723.94	142.5	285	-	-	40.5

2.3 Methods

To evaluate the mechanical properties of the AACs, both cubic (50x50x50 mm) and prismatic (40x40x160 mm) samples were prepared. Compressive and flexural strengths were measured using an automatic testing machine following the relevant standards. For water absorption tests, as per ASTM C 642, the oven-dried samples were weighed and then immersed in water for 48 hours to achieve saturation before being reweighed. Flexural strength was assessed on the 28th day using a single-point loading method in a standardized testing setup

3. Results and Discussion

3.1 Physical Properties

Water absorption remains high at a 2.0% fiber ratio, indicating that further increases in fiber content do not effectively reduce water absorption. The sustained high water absorption at a 2.0% fiber ratio indicates a saturation point at which additional fibers contribute more to porosity than water absorption. This phenomenon may be attributed to the fibers exceeding the optimal concentration, resulting in a poorly compacted matrix with increased voids. These observations underscore the significance of maintaining an optimal fiber ratio to minimize water absorption and enhance the durability of AACs. The optimal fiber ratio, as indicated by the graph, appears to be approximately 1.0%, where water absorption is significantly reduced, suggesting a well-compacted and dense matrix. Porosity, defined as the volume fraction of voids within a material, is a crucial determinant of its mechanical properties and durability. Higher porosity is generally correlated with higher water absorption, lower mechanical strength, and increased vulnerability to environmental degradation.

Figure 1 presents the following trends in porosity across different fiber ratios: At a 0.5% fiber ratio, the porosity is relatively high but lower than at higher fiber ratios. This indicates that while the fibers assist in filling some voids, they are not sufficient in creating a significantly denser matrix. The moderate porosity indicates that at a 0.5% fiber ratio, the fibers are somewhat effective in enhancing the matrix structure but not to the extent required for substantial porosity reduction. A notable decrease in porosity is observed at a 1.0% fiber ratio, which correlates with the reduced water absorption at this ratio. The substantial reduction in porosity indicates that the fibers are effectively distributed within the matrix, filling the voids and creating a more compact structure. This reduces the number of pathways for water ingress, thereby creating a denser and stronger composite. The 1.0% fiber ratio appears to be the optimal concentration for achieving low porosity, enhancing AACs' mechanical and durability properties.

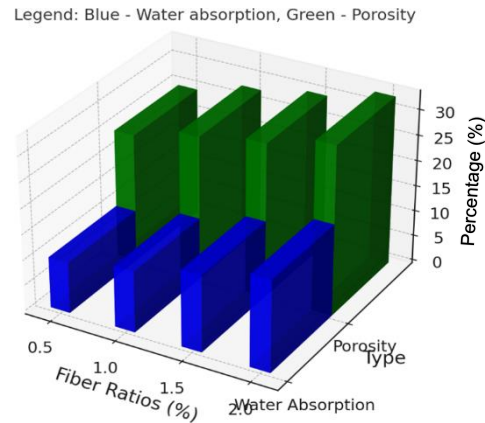


Figure 1 – Water absorption and void ratio values of fiber-reinforced AACs at 28 days

The high porosity observed at a 1.5% fiber ratio illustrates the harmful effects of an excessive fiber content in the absence of adequate dispersion. The porosity slightly declines from the peak observed at a 1.5% fiber ratio yet remains elevated relative to the levels observed at lower fiber contents. The slight decrease in porosity indicates that while some improvement is observed, the distribution and interaction of fibers within the matrix remain suboptimal. The sustained high porosity at a 2.0% fiber ratio indicates that the matrix remains compromised by fiber agglomeration and increased void content. These observations underscore the necessity for a delicate balance in fiber reinforcement. The optimal fiber content enhances the density of the matrix and reduces porosity. Conversely, excessive fiber content leads to agglomeration, increased voids, and higher porosity. The graph indicates that the optimal fiber ratio for minimizing porosity is approximately 1.0%, which aligns with the trends observed for water absorption. Incorporating AS and various fiber types further refines the understanding of AAC properties. The study indicates that incorporating 10% and 20% AS in the AAC matrix significantly reduces water absorption. This reduction is attributed to the chemical interactions facilitated by the CaO/CaSO₄ composite activator. These interactions result in the formation of long-chain Si-O-Al-O structures, which reduce porosity and enhance matrix density. However, at 30% AS, water absorption increases, likely due to oversaturation and the resultant microstructural weaknesses. This suggests a threshold beyond which additional AS no longer contributes positively has been reached. The fibers play a pivotal role in determining the water absorption and porosity of the material. Among the fiber-reinforced AACs, BFs demonstrate the lowest water absorption and void values across all ratios, indicating their superior interaction and reinforcement capabilities within the AAC matrix. PEF at 1% yields the highest unit weight, suggesting significant matrix densification. In contrast, PAFs show less impact on unit weight but contribute to reducing water absorption and porosity at optimal ratios. The findings of this study align with those of Sahin et al. [3], who previously examined the durability parameters related to water absorption and porosity of 56-day AAC samples. The study found that porosity decreased rapidly with a 0.4% PEF ratio, but the rate of decrease slowed with increased PEF ratios. This study's observation that 1% PEF significantly reduces water absorption and porosity aligns with Sahin et al.'s [3] findings, underscoring the importance of optimal fiber concentration for enhancing AAC properties. The comprehensive examination of the water absorption and porosity trends in AAC samples provides crucial insights into optimizing fiber content and aluminum sludge incorporation to develop superior material performance. The optimal fiber ratio of approximately 1.0% significantly reduces water absorption and porosity, creating a dense and durable matrix. However, exceeding this optimal ratio results in the formation of agglomerates, an increase in void content, and higher water absorption and porosity. Incorporating aluminum sludge up to 20% further enhances these properties, while excessive AS content can negate these benefits. BFs demonstrate superior performance across all ratios, indicating their potential for enhancing AACs. These findings provide a comprehensive understanding of the factors influencing AAC properties, thereby guiding the development of high-performance, sustainable construction materials. The highest value of 2.58 g/cm³ was obtained in the

1% PEF series (Figure 1), as indicated by the unit weights of the AAC samples. Although the unit weight did not change significantly with PAF-reinforcement, an increase in unit weight was observed with BF-reinforcement, although to a limited extent. The study observed a sharp decrease in water absorption values when 10% and 20% AS were included in the C series, but the water absorptions increased when 30% AS was added. This phenomenon can be attributed to the influence of the CaO/CaSO₄ composite activator, which continues to depolymerize and recombine the chemical bonds of Al-O and Si-O, ultimately forming long-chain AS-based AACs. Correlation analysis revealed that incorporating 0.5% PAF reinforcement, 0.5% BF reinforcement into the AAC samples resulted in a reduction in water absorption and void ratios and increased unit weights. BF exhibited the lowest water absorption and void values for all ratios among the fiber-reinforced AACs. The study by Sahin et al. [3] examined the durability parameters related to water absorption and porosity of the 56-day AAC samples. It is argued that the porosity decreased rapidly when the PEF ratio was 0.4%, but the rate of decrease in the porosity slowed with the increase in the PEF ratio. It is well established that the type, ratio, and distribution of pores in concrete have a detrimental impact on dimensional stability, strength, and durability properties. This phenomenon was mitigated by incorporating PEF into the composites, preventing microcracks formation.

3.2 Mechanical Properties

Before further testing, trial mixtures were prepared with varying compositions and molarity ratios. The series exhibiting the highest compressive and flexural strengths were selected for detailed physical and mechanical property evaluations. Subsequent experiments were conducted to investigate the effects of adding 10%, 20%, and 30% AS to the optimized series.

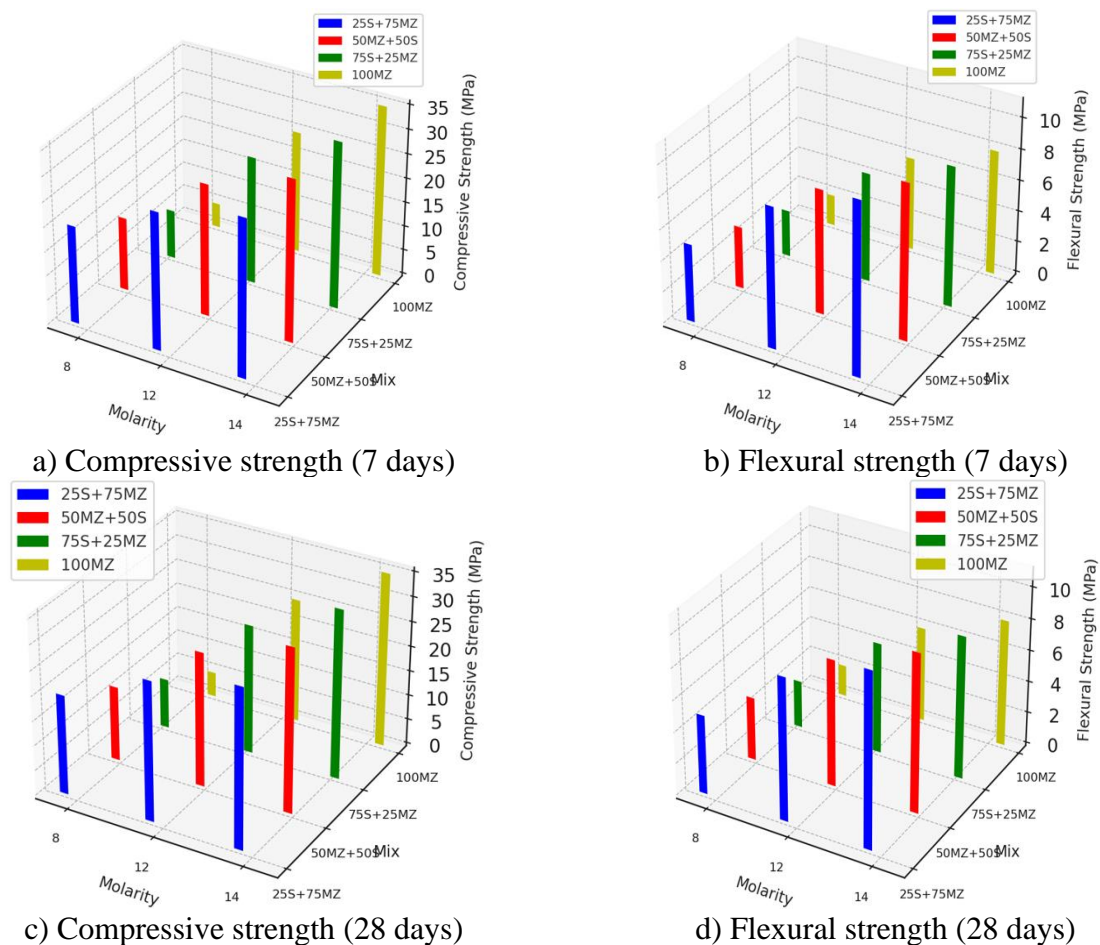
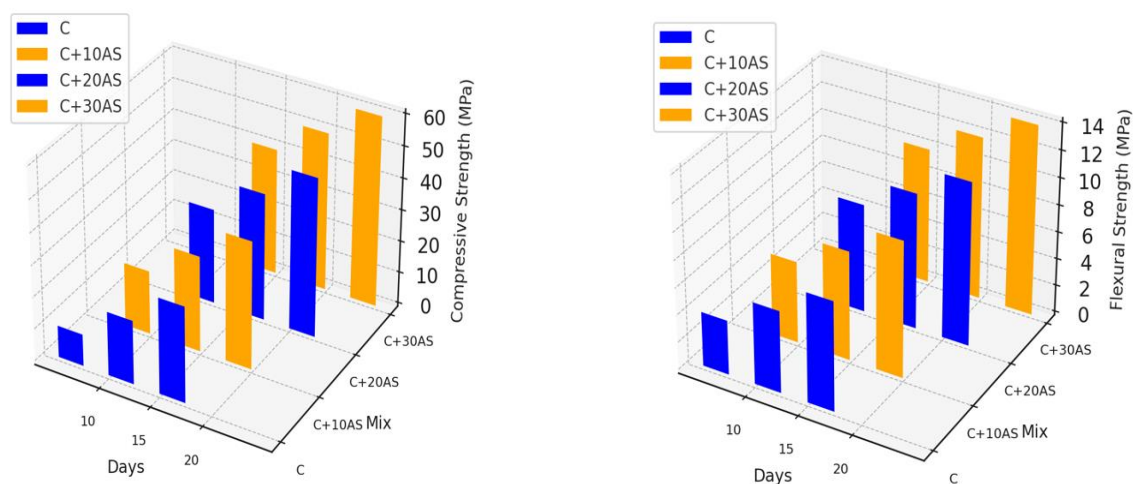


Figure 2 – Compressive and flexural strengths of AACs of different molarity and mixing ratios at 7 and 28 days

Figures 2a and 2c illustrate the anticipated positive correlation between NaOH concentration and compressive and flexural strengths, with peaks observed at 12M before a slight decline at 14 M. Similar trends have been observed by Malkawi et al. [32], Chaithanya et al. [33] in AACs containing fly ash (FA) or S. These findings are consistent with those of Singh et al. [34] and Mudgal et al. [35], who also identified optimal AS levels for improved strength and compactness in AACs. The presence of AS is conducive to geopolymerization, which likely contributes to a higher Si/Al and Na/Al molar ratio, thereby enhancing densification and strength. Aygörmez [36, 37] reported similar improvements in AAC mortars, achieving a 12% increase in compressive strength with 25% AS replacement. Notably, Zakira et al. [38] achieved even higher strengths (66 MPa) using 50% AS, highlighting AS's potential for high-performance AACs. The data indicates that the presence of AS in varying percentages significantly influences AACs' compressive and flexural strengths, suggesting that it plays a pivotal role in the geopolymer matrix. The study's results are consistent with previous findings that higher concentrations of NaOH facilitate the dissolution of aluminosilicate materials, thereby enhancing the geopolymerization process. However, an excess of NaOH beyond the optimal 12M concentration introduces secondary phases that may not contribute beneficially to the matrix strength. This leads to observed declines at 14M molarity. This phenomenon can be attributed to the oversaturation of alkali ions, which can disrupt the formation of strong, stable aluminosilicate networks, forming weaker structures or even causing microcracking due to excessive alkalinity. The incorporation of AS appears to optimize the internal microstructure of the AACs, promoting a more homogeneous and dense matrix. This densification is of great importance for improving the material's mechanical properties, as it reduces the number of internal voids and enhances the overall bonding within the material. The findings indicate that up to 20% of AS additions result in significant mechanical performance improvements, in alignment with the studies by Singh et al. [34] and Mudgal et al. [35], which reported similar enhancements in AAC properties with optimal AS levels. Beyond this threshold, at 30% AS, the benefits appear to diminish, likely due to the oversaturation effect, which may lead to increased porosity or the formation of less desirable phases within the matrix. This observation highlights the significance of optimizing the content of supplementary materials, such as AS, to balance maximizing strength and maintaining structural integrity. The results of the study on compressive strength over 7 and 28 days and flexural strength over 7 and 28 days demonstrate that the mixture 75S+25MZ with 12M NaOH consistently outperforms other compositions, exhibiting the highest strengths. This is due to the synergistic effects of slag and metazeolite, which provide an optimal balance of reactivity and strength development. The sustained increase in strength over time, particularly in the presence of AS, indicates a stable and ongoing geopolymerization process. This is consistent with the research by Aygörmez [36, 37], which noted significant long-term strength improvements with AS incorporation. The superior performance of the 75S+25MZ mixture at 12M NaOH can be attributed to several factors, including the optimal dissolution of aluminosilicates, the balanced Na/Al and Si/Al ratios, and the effective densification of the matrix. The presence of slag contributes to long-term strength due to its latent hydraulic properties, which continue to enhance the matrix even after the initial curing period. This is consistent with the findings of Chaithanya et al. [33], who also observed long-term strength gains in AACs with slag. The incorporation of fibers at specific ratios enhances the material's mechanical properties, as it improves the internal bonding and reduces microcracking. The findings indicate that a 1.0% fiber ratio is optimal for compressive and flexural strengths, providing the optimal balance between fiber reinforcement and matrix integrity. The positive correlation between NaOH concentration and mechanical properties up to 12M is well-supported by the literature, with similar trends observed in studies by Malkawi et al. [32] and Singh et al. [34]. The slight decline at 14M further reinforces the necessity of optimizing alkali concentrations to prevent harmful effects on the matrix structure. The influence of AS on the microstructure is also crucial, as it promotes a more cohesive and dense matrix, enhancing both strength and durability. AACs' compressive strength at seven days significantly depends on the NaOH solution's molarity and the mixture composition. The 75S+25MZ mixture exhibits the highest compressive strength across all molarity levels, particularly at 12M, reaching approximately 50 MPa.

This high early strength indicates an efficient geopolymerization process facilitated by the optimal Si/Al and Na/Al ratios, which enhance the matrix density and reduce porosity. The observed trend of increasing strength with higher molarity up to 12M is consistent with the findings of Malkawi et al. [32], who reported that higher NaOH concentrations improve the dissolution of aluminosilicate precursors, leading to a denser and stronger matrix. Nevertheless, the slight decline in strength at 14M may be attributed to the excessive alkali content, which may result in the formation of alkali carbonates or other secondary phases that do not contribute to strength development. At 28 days, the compressive strength trends remain consistent with the 7-day results. The 75S+25MZ mixture performs better, achieving compressive strengths exceeding 50 MPa at 12M NaOH. This sustained strength gain over time indicates a stable and ongoing geopolymerization process. Slag in the mixture enhances the long-term strength due to its latent hydraulic properties, which contribute to continued strength development beyond the initial curing period. Similarly, Chaithanya et al. [33] observed comparable long-term strength gains in AACs with S, underscoring the significance of slag content in attaining high-performance composites. Flexural strength is a crucial parameter that reflects the material's capacity to withstand bending and cracking. The flexural strength at seven days follows a similar trend to compressive strength, with the 75S+25MZ mixture exhibiting the highest values. At 12M NaOH, the flexural strength reaches approximately 18 MPa, highlighting the beneficial effects of this specific mixture composition. The enhanced flexural strength can be attributed to the improved bonding between the fibers and the geopolymer matrix, which enhances load transfer and crack resistance. This finding is consistent with the findings of Singh et al. [34], who reported that optimal AS levels and fiber reinforcement significantly enhance the flexural strength of AACs. The 28-day flexural strength results serve to reinforce the superiority of the 75S+25MZ mixture. At 12M NaOH, the flexural strength exceeds 20 MPa, indicating excellent durability and resistance to bending stresses over time. The slight decline observed at 14M molarity is consistent with the compressive strength results, suggesting that excessively high NaOH concentrations may harm the matrix structure. Mudgal et al. [35] also observed that while higher alkali concentrations enhance early strength, they can lead to long-term durability issues if not optimized. The presence of AS in the AAC matrix significantly enhances the mechanical properties, promoting geopolymerization and densification. The study indicates that incorporating 10% and 20% AS into the AAC matrix reduces water absorption. This is attributed to the chemical interactions facilitated by the CaO/CaSO₄ composite activator. These interactions result in the formation of long-chain Si-O-Al-O structures, which reduce porosity and enhance matrix density. However, at 30% AS, water absorption increases, likely due to oversaturation and the resultant microstructural weaknesses. This suggests a threshold beyond which additional AS no longer contributes positively has been reached.



a) Compressive strength (7-28 days)

b) Flexural strength (7-28 days)

Figure 3 – Compressive and flexural strengths of AACs in different AS ratios at 7 and 28 days

The series with the highest compressive strength was identified by adding 30% AS. Various ratios and types of synthetic fiber reinforcements were utilized to enhance the performance, as depicted in Figure 3. The data presented in Figure 4 indicates that PEFs were beneficial only up to a 1% addition, achieving a maximum compressive strength of 47.06 MPa before experiencing a significant decline. This decline can be attributed to fiber agglomeration at higher concentrations, which leads to poor dispersion and the creation of weak points within the matrix. Conversely, the results for PAF and BFs were the most favorable at a 0.5% addition, with compressive strengths of 56.36 MPa for PA and 61.85 MPa for BF, exceeding those of the control mix. The 7.03% increase for BF can be attributed to its superior crack bridging capabilities and bond strength with the matrix. The fibers form a three-dimensional network within the matrix, preventing transverse deformations and inhibiting the propagation of microcracks. The fiber bridging effect and the strong bond strength between the fibers and the AAC matrix achieve this crack formation control. Incorporating fibers at specific ratios is crucial for optimizing mechanical properties, as it improves internal bonding and reduces microcracking. The findings of this study are consistent with those of Sahin et al. [3], who investigated metakaolin (MK)--based AACs reinforced with PEFs and observed similar trends, namely that mechanical properties improved up to an optimal fiber concentration. Subsequently, the benefits declined due to the formation of fiber agglomerates. Similarly, Uysal et al. [39] observed enhancements in mechanical properties with various fibers in AS-MK-AACs. The researchers observed that PVAFs effectively increased flexural strength by 61% compared to the control, indicating the potential of synthetic fibers to enhance AACs' mechanical performance. The enhanced performance of BFs can be attributed to their intrinsic properties and the synergistic interactions with the AAC matrix. BFs from volcanic rock exhibit excellent mechanical properties, including high tensile strength, chemical resistance, and thermal stability. These properties render BFs particularly suitable for reinforcing AACs, as they can withstand the alkaline environment and high temperatures associated with geopolymerization. The compatibility of BFs with the AAC matrix ensures effective stress transfer and crack bridging, which results in insignificantly improved strength. The fiber bridging effect, whereby fibers span across cracks and transfer stress, is pivotal in regulating crack formation and development. As the fibers bridge the cracks, they effectively arrest crack growth and enhance the load-bearing capacity of the AACs. This mechanism is particularly significant in preventing catastrophic failure and enhancing the material's durability. Another crucial factor is the bond strength between the fibers and the matrix, which determines the stress transfer efficiency from the matrix to the fibers. BFs, with their superior bonding characteristics, contribute to forming a more cohesive and resilient matrix. Nevertheless, an increase in fiber content can result in a reduction in the workability of AACs. Concentrations of fibers over a certain threshold may result in the formation of agglomerates, wherein the fibers aggregate in a manner that is not uniform throughout the matrix. The clustering of fibers within the AACs results in the formation of weak points and voids, subsequently reducing the material's strength. It is paramount to strike a balance between the fiber content and the workability of the material, as an excess of fibers can harm the overall performance of the material. This underscores the necessity of achieving an optimal fiber ratio to attain the desired mechanical properties without compromising workability. The study's results on compressive strength over 7 and 28 days, as illustrated in Figure 3, demonstrate that the mixture with 30% AS consistently outperforms other compositions, exhibiting the highest strengths. This is due to the synergistic effects of slag and metazeolite, which provide an optimal balance of reactivity and strength development. The sustained strength gain over time, particularly in the presence of AS, indicates a stable and ongoing geopolymerization process. This is consistent with the research by Aygörmez [36, 37], which noted significant long-term strength improvements with AS incorporation. The superior performance of the 30% AS mixture can be attributed to several factors, including the optimal dissolution of aluminosilicates, the balanced Na/Al and Si/Al ratios, and the effective densification of the matrix. The presence of slag contributes to long-term strength due to its latent hydraulic properties, which continue to enhance the matrix even after the initial curing period. This is consistent with the findings of Chaithanya et al. [33], who also observed long-term strength gains

in AACs with slag. As depicted in Figure 4, the flexural strength results further confirm the benefits of fiber reinforcement in AACs. Incorporating PA and BF fibers at optimal concentrations markedly enhances flexural strength, conferring superior resistance to bending stresses. The enhanced flexural strength can be attributed to the improved bonding between the fibers and the AAC matrix, which enhances load transfer and crack resistance. This finding is consistent with the findings of Singh et al. [34], who reported that optimal AS levels and fiber reinforcement significantly improve the flexural strength of AACs. Forming a three-dimensional network within the AAC matrix by the fibers is critical for enhancing mechanical properties. This network not only improves load transfer but also contributes to the overall toughness of the material. Toughness, the capacity to absorb energy and deform plastically before fracturing, is a fundamental property of construction materials subjected to dynamic and impact loads. Incorporating fibers into AACs enhances their toughness by providing multiple crack-bridging sites, thereby delaying crack propagation and increasing the material's energy absorption capacity. Moreover, the bond strength between the fibers and the matrix is of critical importance for the effectiveness of fiber reinforcement. Adequate bond strength ensures that the fibers can effectively transfer stress from the matrix, thereby enhancing the overall load-bearing capacity of the AACs. BFs, with their superior bond strength, facilitate the formation of a more cohesive and resilient matrix, thereby leading to significant improvements in compressive strength. Several factors, including the fibers' surface characteristics, the matrix's composition, and the curing conditions, influence the interfacial bond between the fibers and the matrix. The optimization of these factors can further enhance the bond strength and overall performance of fiber-reinforced AACs.

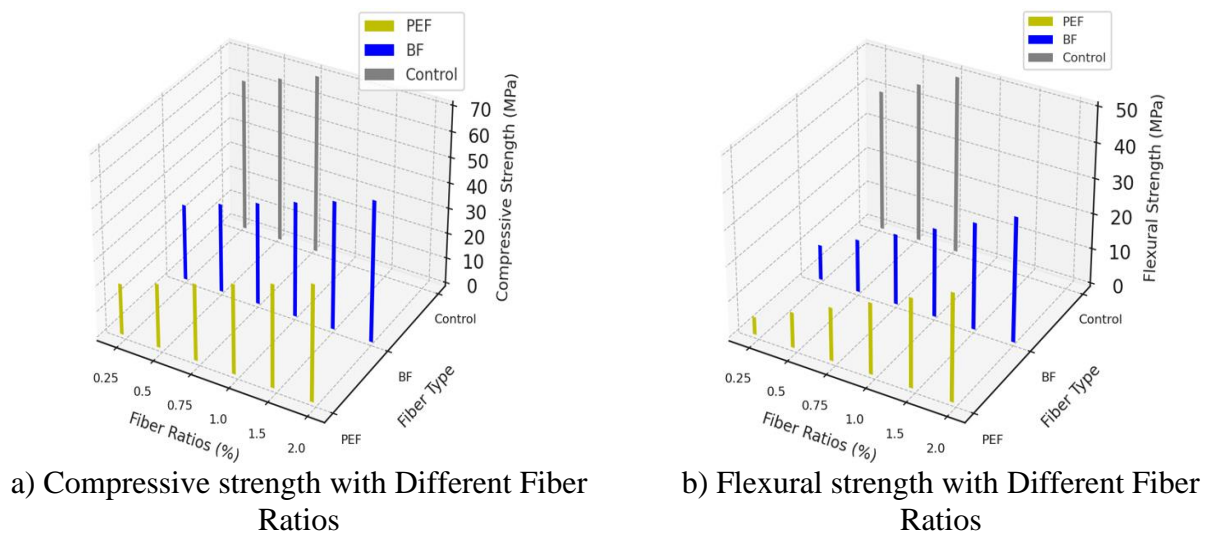


Figure 4 – Compressive and flexural strengths of AACs in different synthetic fibers and ratios at 28 days

The incorporation of synthetic fibers, including PEFs, PAFs, and BFs, significantly impacted the mechanical properties of AACs in comparison to the control samples. The flexural strength of the composites increased modestly with fiber reinforcement, with an improvement of approximately 0.5% observed for both PEF and PAF at a fiber content of 0.5%. However, incorporating BF at the same 0.5% ratio yielded a substantial improvement of 12.61%, highlighting the superior reinforcing capabilities of BFs. Notably, when the PEF content was increased to 1%, the flexural strength exhibited a higher value of 10.54 MPa. Notwithstanding this increase, the strength remained below the control value of 12.34 MPa. This trend indicates that while PEFs can enhance flexural strength at certain ratios, they may not be as effective as other fibers, such as BF, especially at higher concentrations. The observed pattern of initial strength increase followed by a decline at higher fiber contents is consistent with findings from other studies, including those by Alomayri et al. [40, 41], who investigated cotton fiber-reinforced FA-based AACs (FA-AACs). A similar trend was observed, whereby the flexural strength initially increased with fiber content up to 0.5% but declined beyond

this point. This behavior can be attributed to optimal fiber dispersion at lower ratios, facilitating effective stress transfer. In contrast, higher fiber contents can lead to accumulation and inhomogeneous distribution within the matrix. The superior performance of BF at 0.5% can be attributed to its intrinsic mechanical properties and its interaction with the AAC matrix. BFs are renowned for their high tensile strength, excellent chemical resistance, and thermal stability, rendering them optimal for reinforcing AACs. The robust bond between BFs and the AAC matrix ensures efficient stress transfer and crack bridging, significantly enhancing the material's flexural strength. This is corroborated by the findings of Baykara et al. [42], who observed that PPF-reinforced AACs also exhibited optimal performance at 0.5% fiber content. Beyond this optimal ratio, the performance declined due to potential issues such as fiber inhomogeneity and agglomeration, which compromise the matrix integrity and form weak points. The reinforcement mechanism of fibers in AACs can be understood through several key factors, including fiber-matrix bonding, fiber dispersion, and the mechanical properties of the fibers themselves. The bond strength between the fibers and the matrix is paramount for effectively transferring loads. In the case of BF, the high bond strength with the AAC matrix ensures that the fibers can effectively bridge cracks and transfer stress, thereby enhancing the overall mechanical properties. Another crucial factor is the dispersion of fibers within the matrix. The fibers are more likely to be uniformly distributed at lower fiber contents, thereby providing effective reinforcement. However, as the fiber content increases, the likelihood of fiber agglomeration also increases, which can lead to an inhomogeneous distribution and the formation of weak zones within the composite. This phenomenon can be attributed to the decline in mechanical properties observed at higher fiber contents. Moreover, the mechanical properties of the fibers themselves play a significant role in the overall performance of the composite. BFs, with their high tensile strength and modulus of elasticity, are particularly effective in enhancing the flexural strength of AACs. The capacity of BF to establish a three-dimensional network within the matrix facilitates the control of crack propagation and enhances the material's toughness. This three-dimensional network not only bridges cracks but also provides multiple pathways for stress transfer, thereby improving the load-bearing capacity and durability of the composite. The influence of fiber type and content on the mechanical properties of AACs can also be analyzed through the lens of fracture mechanics. The incorporation of fibers within the matrix alters the fracture behavior of the composite. Fibers act as barriers to crack propagation, increasing the energy required for crack growth and thereby improving the toughness and flexural strength of the composite. In the case of BF-reinforced AACs, the strong fiber-matrix bond and the high tensile strength of BF contribute to a significant increase in flexural strength, as evidenced by the 12.61% improvement observed in this study. The optimal performance observed at 0.5% fiber content for both PEF and BF indicates a critical fiber content beyond which the negative effects of fiber agglomeration and inhomogeneous distribution outweigh the benefits of fiber reinforcement. The critical content varies depending on the type of fiber and its interaction with the matrix. The decline in flexural strength observed for PEF can be attributed to forming fiber clusters, which act as stress concentrators and initiate crack formation. For BF, the decline at higher contents can be linked to the same issues, although the intrinsic properties of BF allow it to maintain higher performance at lower contents. Furthermore, the study underscores the significance of elucidating the cooperative effects of diverse components in the composite. The combination of MZ, S, AS, and RCA forms a complex matrix with unique properties. Adding fibers introduces another level of complexity, as the interaction between fibers and the matrix can significantly influence the mechanical properties. The optimal combination of these components can result in the development of high-performance, sustainable construction materials.

In conclusion, the reinforcement of AACs with synthetic fibers, such as PEF, PAF, and BF, significantly influences the mechanical properties of the composites. The study demonstrates that BF at a 0.5% addition provides the most substantial improvement in flexural strength, attributed to its superior mechanical properties and strong bond with the AAC matrix. The observed trends of initial strength improvement followed by a decline in higher fiber contents are consistent with findings from other studies. They can be explained by fiber dispersion, aggregation, and fiber-matrix bonding.

These findings underscore the importance of optimizing fiber content and type to achieve the desired mechanical properties in AACs. The findings of this study can inform the development of high-performance, eco-friendly construction materials that meet modern performance standards.

The reinforcement of AACs with synthetic fibers represents a promising approach to enhancing the mechanical properties of these composites. The findings of this study provide valuable insights into the optimal fiber content and type for achieving superior performance. Future research should further explore the synergistic effects of different fiber types and supplementary materials to develop advanced AACs with enhanced mechanical properties and durability. By elucidating the intricate interactions between fibers and the matrix, researchers can devise composites that fulfill and exceed contemporary construction applications' demands. The potential of MZ-S-based AACs with AS and BF to create sustainable, high-performance construction materials is considerable, and this study establishes a foundation for future innovations in this field.

4. Conclusions

The study explores the effects of varying concentrations of materials such as metakaolin (MZ), slag (S), and alkaline solution (AS), as well as the incorporation of basalt fibers (BF) and polyethylene fibers (PEF) on the mechanical properties of AAC. The results demonstrate significant improvements in compressive and flexural strengths, optimal material ratios for enhanced performance, and the impact of fiber content on the overall integrity of the composite matrix:

1. Optimal AAC mix, comprising 50% MZ and 50% S, was activated with 12M NaOH and enhanced with 30% AS. This resulted in a significantly higher compressive strength than in mixes without AS. Adding 0.5% BF resulted in a notable enhancement in compressive strength, reaching 61.85 MPa from the baseline of 52.57 MPa. This represents a substantial improvement of 9.28 MPa.

2. Adding 0.5% BF to the mix significantly increased the flexural strength, reaching 18.15 MPa, an increase of 3.53 MPa from the initial value of 14.62 MPa. The mixture with 1% PEF reached a flexural strength of 10.54 MPa. This showed that it was insufficient to exceed the flexural strength of the control mixture of 12.34 MPa.

3. Incorporating of 10% AS into the mixture reduced water absorption to 5.2%, a value significantly lower than the 7.5% observed in control. This reduction in water absorption led to an enhancement in material density. An increase in AS content to 20% further reduced water absorption to 3.8%, indicating a substantial improvement in resistance to water ingress. However, at 30% AS content, water absorption slightly increased to 4.5%, suggesting that a saturation point may have been reached beyond which additional AS no longer improves performance.

4. Fiber concentrations above 1% led to aggregation, reducing mechanical properties by approximately 10% due to forming weak zones within the matrix.

AACs exhibit superior mechanical properties, with a compressive strength of 61.85 MPa, in comparison to the strength of OPCs, which typically range from 30 to 50 MPa, with a flexural strength of up to 18.15 MPa, which is considerably higher than the range of 3 to 5 MPa observed in OPCs. Regarding durability, AACs exhibit low water absorption values, with 20% AS content resulting in values of approximately 4%. This contrasts OPC, which exhibits values of 6% to 10%. This difference in water absorption indicates a denser and less porous matrix, which results in increased long-term durability and resistance to environmental factors such as freeze-thaw cycles and chemical attacks. Additionally, the AAC formulation combining RCA and AS addresses waste management issues and facilitates sustainable construction practices by reducing the demand for virgin raw materials. This is consistent with global sustainability goals and facilitates a circular economy in the construction industry. The comprehensive benefits of AAC, including superior mechanical performance, increased durability, and significant environmental advantages, position these building materials as a highly competitive and environmentally friendly alternative to existing materials. These findings demonstrate the transformative potential of AAC formulation in the development of sustainable and high-performance construction materials.

Acknowledgments

This work was supported by the research fund of the Scientific and Technological Research Council of Turkey (TUBITAK), the authors would like to express their sincere gratitude to scientific research coordination unit for their financial support to the project (Project number: 123M288).

References

1. Combined effect of using steel fibers and demolition waste aggregates on the performance of fly ash/slag based geopolymer concrete / A.M. Lakew, O. Canpolat, M.M. Al-Mashhadani, M. Uysal, A. Niş, Y. Aygörmmez, M. Bayati // *European Journal of Environmental and Civil Engineering*. — 2023. — Vol. 27, No. 15. — P. 4251–4278. <https://doi.org/10.1080/19648189.2023.2189468>
2. Erken Yaşdaki Atık Betonların Geri Dönüşüm Agregası Olarak Beton Üretiminde Kullanılabilirliği ve Sürdürülebilirlik Açısından İncelenmesi / C. Demirel, O. Şimşek // *Düzce Üniversitesi Bilim ve Teknoloji Dergisi*. — 2015. — Vol. 3, No. 1. — P. 226–235.
3. The effect of polyvinyl fibers on metakaolin-based geopolymer mortars with different aggregate filling / F. Sahin, M. Uysal, O. Canpolat, T. Cosgun, H. Dehghanpour // *Construction and Building Materials*. — 2021. — Vol. 300. — P. 124257. <https://doi.org/10.1016/j.conbuildmat.2021.124257>
4. Frost resistance of internal curing concrete with calcined natural zeolite particles / X. Zheng, J. Zhang, X. Ding, H. Chu, J. Zhang // *Construction and Building Materials*. — 2021. — Vol. 288. — P. 123062. <https://doi.org/10.1016/j.conbuildmat.2021.123062>
5. Effects of calcination and milling pre-treatments on natural zeolites as a supplementary cementitious material / C. Florez, O. Restrepo-Baena, J.I. Tobon // *Construction and Building Materials*. — 2021. — Vol. 310. — P. 125220. <https://doi.org/10.1016/j.conbuildmat.2021.125220>
6. Optimization of geopolymers based on natural zeolite clinoptilolite by calcination and use of aluminate activators / A. Nikolov, H. Nugteren, I. Rostovsky // *Construction and Building Materials*. — 2020. — Vol. 243. — P. 118257. <https://doi.org/10.1016/j.conbuildmat.2020.118257>
7. Compressive Strength and Microstructural Characteristics of Natural Zeolite-based Geopolymer / S. Özen, B. Alam // *Periodica Polytechnica Civil Engineering*. — 2017. <https://doi.org/10.3311/PPci.10848>
8. Performance of ambient and freezing-thawing cured metazeolite and slag based geopolymer composites against elevated temperatures / Y. Aygörmmez // *Revista de la construcción*. — 2021. — Vol. 20, No. 1. — P. 145–162. <https://doi.org/10.7764/RDLC.20.1.145>
9. Influence of steel and PP fibers on mechanical and microstructural properties of fly ash-GGBFS based geopolymer composites / R.R. Bellum // *Ceramics International*. — 2022. — Vol. 48, No. 5. — P. 6808–6818. <https://doi.org/10.1016/j.ceramint.2021.11.232>
10. Improving the Mechanical Strengths of Hybrid Waste Geopolymer Binders by Short Fiber Reinforcement / O.A. Abdulkareem, J.C. Matthews // *Arabian Journal for Science and Engineering*. — 2021. — Vol. 46, No. 5. — P. 4781–4789. <https://doi.org/10.1007/s13369-020-05170-6>
11. Tensile behavior and microstructure of hybrid fiber ambient cured one-part engineered geopolymer composites / Y. Alrefaei, J.-G. Dai // *Construction and Building Materials*. — 2018. — Vol. 184. — P. 419–431. <https://doi.org/10.1016/j.conbuildmat.2018.07.012>
12. Development of Coconut Trunk Fiber Geopolymer Hybrid Composite for Structural Engineering Materials / F. Amalia, N. Akifah, Nurfadilla, Subaer // *IOP Conference Series: Materials Science and Engineering*. — 2017. — Vol. 180. — P. 012014. <https://doi.org/10.1088/1757-899X/180/1/012014>
13. Mechanical and durability characterization of hybrid fibre reinforced green geopolymer concrete / K. Arunkumar, M. Muthukannan, A. Sureshkumar, A. Chithambarganesh // *Research on Engineering Structures and Materials*. — 2021. — Vol. 8, No. 1. — P. 19–43. <https://doi.org/10.17515/resm2021.280mal604>
14. Enhancement of mechanical properties of fly ash geopolymer containing fine recycled concrete aggregate with micro carbon fiber / P. Nuaklong, A. Wongsak, K. Boonserm, C. Ngohpok, P. Jongvivatsakul, V. Sata, P. Sukontasukkul, P. Chindaprasirt // *Journal of Building Engineering*. — 2021. — Vol. 41. — P. 102403. <https://doi.org/10.1016/j.jobbe.2021.102403>
15. Mechanical properties, microstructure and drying shrinkage of hybrid fly ash-basalt fiber geopolymer paste / W. Punurai, W. Kroehong, A. Saptamongkol, P. Chindaprasirt // *Construction and Building Materials*. — 2018. — Vol. 186. — P. 62–70. <https://doi.org/10.1016/j.conbuildmat.2018.07.115>
16. Compressive Strength Development of Slag-Based Geopolymer Paste Reinforced with Fibers Cured at Ambient Condition / W.H. Sachet, W.D. Salman // *IOP Conference Series: Materials Science and Engineering*. — 2020. — Vol. 928, No. 2. — P. 022117. <https://doi.org/10.1088/1757-899X/928/2/022117>
17. Evaluation of properties of steel fiber reinforced GGBFS-based geopolymer composites in aggressive environments / K. Zada Farhan, M. Azmi Megat Johari, R. Demirboğa // *Construction and Building Materials*. — 2022. — Vol. 345. — P. 128339. <https://doi.org/10.1016/j.conbuildmat.2022.128339>
18. Impact of Flax and Basalt Fibre Reinforcement on Selected Properties of Geopolymer Composites / M. Frydrych, Š. Hýsek, L. Fridrichová, S. Le Van, M. Herlík, M. Pechočiaková, H. Le Chi, P. Louda // *Sustainability*. — 2019. — Vol. 12, No. 1. — P. 118. <https://doi.org/10.3390/su12010118>

19. Evaluation of hybrid steel fiber reinforcement in high performance geopolymer composites / X. Gao, Q.L. Yu, R. Yu, H.J.H. Brouwers // *Materials and Structures*. — 2017. — Vol. 50, No. 2. — P. 165. <https://doi.org/10.1617/s11527-017-1030-x>
20. Effect of high-temperature on the behavior of single and hybrid glass and basalt fiber added geopolymer cement mortars / S. Guler, Z.F. Akbulut // *Journal of Building Engineering*. — 2022. — Vol. 57. — P. 104809. <https://doi.org/10.1016/j.jobe.2022.104809>
21. Investigation on Flexural Behavior of Geopolymer-Based Carbon Textile/Basalt Fiber Hybrid Composite / C.H. Le, P. Louda, K. Ewa Buczkowska, I. Dufkova // *Polymers*. — 2021. — Vol. 13, No. 5. — P. 751. <https://doi.org/10.3390/polym13050751>
22. Effect of Hybrid Fibres on the Durability Characteristics of Ternary Blend Geopolymer Concrete / V. Sathish Kumar, N. Ganesan, P.V. Indira // *Journal of Composites Science*. — 2021. — Vol. 5, No. 10. — P. 279. <https://doi.org/10.3390/jcs5100279>
23. Development and Characterization of Lightweight Geopolymer Composite Reinforced with Hybrid Carbon and Steel Fibers / A. Baziak, K. Pławecka, I. Hager, A. Castel, K. Korniejenco // *Materials*. — 2021. — Vol. 14, No. 19. — P. 5741. <https://doi.org/10.3390/ma14195741>
24. Experimental Study on the Behaviour of Hybrid Fiber Reinforced Geopolymer Concrete under Ambient Curing Condition / A. Chithambar Ganesh, M. Muthukannan // *IOP Conference Series: Materials Science and Engineering*. — 2019. — Vol. 561. — P. 012014. <https://doi.org/10.1088/1757-899X/561/1/012014>
25. Short SiC Fiber and Hybrid SiC/Carbon Fiber Reinforced Geopolymer Matrix Composites / D. Jia, P. He, M. Wang, S. Yan // *Geopolymer and Geopolymer Matrix Composites: Vol. 311: Springer Series in Materials Science*. — Singapore: Springer Singapore, 2020. — P. 243–270. https://doi.org/10.1007/978-981-15-9536-3_7
26. Workability and Flexural Properties of Fibre-Reinforced Geopolymer Using Different Mono and Hybrid Fibres / J. Junior, A.K. Saha, P.K. Sarker, A. Pramanik // *Materials*. — 2021. — Vol. 14, No. 16. — P. 4447. <https://doi.org/10.3390/ma14164447>
27. Tensile and flexural strength cracking behavior of geopolymer composite reinforced with hybrid fibers / M.M. Maras // *Arabian Journal of Geosciences*. — 2021. — Vol. 14, No. 22. — P. 2258. <https://doi.org/10.1007/s12517-021-08579-x>
28. Flexural performance and toughness of hybrid steel and polypropylene fibre reinforced geopolymer / P. Sukontasukkul, P. Pongsopha, P. Chindaprasirt, S. Songpiriyakij // *Construction and Building Materials*. — 2018. — Vol. 161. — P. 37–44. <https://doi.org/10.1016/j.conbuildmat.2017.11.122>
29. A feasibility of enhancing the impact resistance of hybrid fibrous geopolymer composites: Experiments and modelling / N.P. Asrani, G. Murali, K. Parthiban, K. Surya, A. Prakash, K. Rathika, U. Chandru // *Construction and Building Materials*. — 2019. — Vol. 203. — P. 56–68. <https://doi.org/10.1016/j.conbuildmat.2019.01.072>
30. Effects of fiber hybridization on mechanical properties and autogenous healing of alkali-activated slag-based composites / J.-I. Choi, H.H. Nguyễn, S.-E. Park, R. Ranade, B.Y. Lee // *Construction and Building Materials*. — 2021. — Vol. 310. — P. 125280. <https://doi.org/10.1016/j.conbuildmat.2021.125280>
31. Tensile and flexural behaviour of recycled polyethylene terephthalate (PET) fibre reinforced geopolymer composites / F.U.A. Shaikh // *Construction and Building Materials*. — 2020. — Vol. 245. — P. 118438. <https://doi.org/10.1016/j.conbuildmat.2020.118438>
32. Effects of Alkaline Solution on Properties of the HCFA Geopolymer Mortars / A.B. Malkawi, M.F. Nuruddin, A. Fauzi, H. Almatarnah, B.S. Mohammed // *Procedia Engineering*. — 2016. — Vol. 148. — P. 710–717. <https://doi.org/10.1016/j.proeng.2016.06.581>
33. Effect Of Molarity On Strength Characteristics Of Geopolymer Mortar Based On Fly ash and GGBS / R. Chaithanya, C. Reddy, L. Reddy, K. Kumar // *Solid State Technology*. — 2021. — Vol. 63. — P. 2020.
34. Performance assessment of bricks and prisms: Red mud based geopolymer composite / S. Singh, M.U. Aswath, R.V. Ranganath // *Journal of Building Engineering*. — 2020. — Vol. 32. — P. 101462. <https://doi.org/10.1016/j.jobe.2020.101462>
35. Fly ash red mud geopolymer with improved mechanical strength / M. Mudgal, A. Singh, R.K. Chouhan, A. Acharya, A.K. Srivastava // *Cleaner Engineering and Technology*. — 2021. — Vol. 4. — P. 100215. <https://doi.org/10.1016/j.clet.2021.100215>
36. Assessment of performance of metabentonite and metazeolite-based geopolymers with fly ash sand replacement / Y. Aygörmez // *Construction and Building Materials*. — 2021. — Vol. 302. — P. 124423. <https://doi.org/10.1016/j.conbuildmat.2021.124423>
37. Evaluation of the red mud and quartz sand on reinforced metazeolite-based geopolymer composites / Y. Aygörmez // *Journal of Building Engineering*. — 2021. — Vol. 43. — P. 102528. <https://doi.org/10.1016/j.jobe.2021.102528>
38. Development of high-strength geopolymers from red mud and blast furnace slag / U. Zakira, K. Zheng, N. Xie, B. Birgisson // *Journal of Cleaner Production*. — 2023. — Vol. 383. — P. 135439. <https://doi.org/10.1016/j.jclepro.2022.135439>
39. The effect of various fibers on the red mud additive sustainable geopolymer composites / M. Uysal, Ö. Faruk Kuranlı, Y. Aygörmez, O. Canpolat, T. Çoşgun // *Construction and Building Materials*. — 2023. — Vol. 363. — P. 129864. <https://doi.org/10.1016/j.conbuildmat.2022.129864>

40. Synthesis and characterization of mechanical properties in cotton fiber-reinforced geopolymer composites / T. Alomayri, I.M. Low // Journal of Asian Ceramic Societies. — 2013. — Vol. 1, No. 1. — P. 30–34. <https://doi.org/10.1016/j.jascer.2013.01.002>
41. Characterisation of cotton fibre-reinforced geopolymer composites / T. Alomayri, F.U.A. Shaikh, I.M. Low // Composites Part B: Engineering. — 2013. — Vol. 50. — P. 1–6. <https://doi.org/10.1016/j.compositesb.2013.01.013>
42. Preparation, characterization, and evaluation of compressive strength of polypropylene fiber reinforced geopolymer mortars / H. Baykara, M.H. Cornejo, A. Espinoza, E. García, N. Ulloa // Heliyon. — 2020. — Vol. 6, No. 4. — P. e03755. <https://doi.org/10.1016/j.heliyon.2020.e03755>

Information about authors:

Ramazan Cingi – PhD Student, Department of Civil Engineering, Istanbul University-Cerrahpasa, Üniversite Yolu No:2, 34320 Avcılar, Istanbul, Turkey, ramazan.cingi@lcwaikiki.com

Bolat Balapanov – PhD Student, Department of Architecture and Construction, Institute of Engineering and Technology, Korkyt Ata Kyzylorda University, Aiteke bi 29 A, Kyzylorda, Kazakhstan, balapanov.sci@gmail.com

Mucteba Uysal – PhD, Professor, Department of Civil Engineering, Yildiz Technical University, Barbaros Bulvarı 34349, Yıldız, Istanbul, Turkey, mucteba@yildiz.edu.tr

Beyza Fahriye Aygun – PhD Student, Department of Civil Engineering, Istanbul University-Cerrahpasa, Üniversite Yolu No:2, 34320 Avcılar, Istanbul, Turkey, beyza.aygun@ogr.iuc.edu.tr

Sarsenbek Montayev – Doctor of Technical Sciences, Professor, Director, Industrial Technological Institute, Zhangir Khan West Kazakhstan Agrarian and Technical University, 51 Zhangir Khan Street, Uralsk, Kazakhstan, montaevs@mail.ru

Orhan Canpolat – PhD, Professor, Department of Civil Engineering, Yildiz Technical University, Barbaros Bulvarı 34349, Yıldız, Istanbul, Turkey, canpolat@yildiz.edu.tr

Author Contributions:

Ramazan Cingi – concept, methodology, resources.

Bolat Balapanov – data collection, funding acquisition, drafting.

Mucteba Uysal – interpretation, analysis.

Beyza Fahriye Aygun – testing, modeling.

Sarsenbek Montayev – visualization.

Orhan Canpolat – editing.

Conflict of Interest: The authors declare no conflict of interest.

Use of Artificial Intelligence (AI): The authors declare that AI was not used.

Received: 04.06.2024

Revised: 15.06.2024

Accepted: 24.06.2024

Published: 26.06.2024



Copyright: © 2024 by the authors. Licensee Technobius, LLP, Astana, Republic of Kazakhstan. This article is an open access article distributed under the terms and conditions of the Creative Commons Attribution (CC BY-NC 4.0) license (<https://creativecommons.org/licenses/by-nc/4.0/>).



Effect of heat treatment of expanded polystyrene concrete on its compressive strength

Murat Rakhimov¹, Galiya Rakhimova¹, Tatyana Samoilo^{1,*}, Nurlan Zhangabay²

¹Department of Construction Materials and Technologies, Abylkas Saginov Karaganda Technical University
Karaganda, Kazakhstan

²Department «Architecture and urban planning», South-Kazakhstan University named after M. Auezov, Shymkent,
Kazakhstan

*Correspondence: tanya.fedulova.18@mail.ru

Abstract. The purpose of this research was to identify the effect of heat treatment of heat-insulating concrete on its compressive strength. For comparison, samples of normal hardening and samples that have undergone heat treatment were used. Lightweight heat-insulating concrete based on cement, polystyrene, and industrial waste was used as the subject of the research. A steaming chamber was used for steaming concrete; tests of the mechanical strength of concrete were carried out on a hydraulic press. All tests were carried out under laboratory conditions. Studies have shown that the density of polystyrene concrete after heat treatment is 7% lower than that of polystyrene concrete hardened under normal conditions. During heat treatment, the crystal structure of the material changes, which affects its final properties. This is proved by the fact that the strength of polystyrene concrete after heat treatment is 30% higher.

Keywords: thermal insulation materials, polystyrene concrete, heat treatment of concrete products, steam chamber, mechanical strength.

1. Introduction

Currently, there are several studies devoted to the production of concrete products without heat treatment [1]. The main goal of these studies is to reduce the cost of finished products by reducing the cost of heating them. However, it seems possible to do this without heat treatment of products under certain environmental temperature conditions. As a rule, the acceptable temperature limit to avoid heat treatment is 20°C. At lower temperatures, the hydration process is significantly reduced, and when water reaches the freezing point, this process stops completely [2]. Given the fact that the production process of thermal insulation products is year-round, in the conditions of the sharply continental climate of the Republic of Kazakhstan, especially in the northern regions of the country, it is not possible to do this without steaming concrete.

It should be noted that much more research has been devoted to steaming heavy concrete, while heat treatment of light concrete has not been studied enough.

The purpose of this research was to identify the effect of heat treatment of heat-insulating concrete on its compressive strength.

To achieve the goal, samples of the same composition were produced, but with different hardening conditions: in a steaming chamber and under normal hardening conditions. Samples in the steaming chamber were subjected to mechanical compressive strength tests immediately after steaming (in less than 1 day), and samples hardening under normal conditions were tested after 1, 3, 7, and 28 days.

There are several factors influencing the rate of hydration:

- Water-Cement ratio (W/C): the low W/C leads to faster hardening in the initial period.

This is because less water in the mixture allows the cement to hydrate faster.

- Mobility: the concrete mixture mobility directly affects the machinery and equipment used in production. A more mobile mixture requires different installation conditions and the use of special equipment.

- Chemical additives: hardening accelerator additives are widely used to accelerate the hardening process [2–4]. They are especially important in cold conditions when the rate of hardening is significantly reduced.

For thermal insulation products, the hardening process must begin before the concrete mixture begins to compact and delaminate. Thus, heat treatment of concrete is an important stage in the production of many thermal insulation products. It improves mechanical properties such as strength, rigidity, and resistance to deformation [5–8].

Another important feature of heat and moisture treatment is its ability to change thermophysical characteristics. These include increased thermal conductivity and decreased heat transfer coefficient. Through heat treatment, the structure of the material changes, which affects its final properties; crystallization and the creation of new phases occur. Heat treatment can improve the material's resistance to high temperatures [9].

The main types of heat treatment include:

- Annealing – prolonged heating at a certain temperature followed by slow cooling. Used to relieve internal stress, improve ductility, and increase corrosion resistance;

- Hardening – rapid cooling after heating to high temperatures. Used to increase hardness and strength;

- Tempering – heating the hardened material to a temperature below the transition point followed by cooling. Used to reduce the fragility of hardened materials;

- Normalization – heating the material to a temperature above the transition point followed by slow cooling in air. It is used to improve the homogeneity of the structure and reduce internal stresses [10].

Heat treatment is used in thermal insulation products with various fillers. Annealing glass wool products improves their mechanical properties and increases resistance to moisture. Annealing basalt wool increases its heat resistance and resistance to deformation. As for the heat treatment of expanded polystyrene, it can be used to increase the strength of the material and at the same time give the material additional porosity. The phenomenon described above is the subject of the study described in this article.

It is important to note that the choice of heat treatment type depends on the thermal insulation material, its purpose, and the required properties. Incorrectly performed heat treatment can lead to the deterioration of the properties of the material. When choosing heat treatment, it is necessary to take into account the characteristics of each specific product. Steaming products in chambers, autoclaves, stands, and forming units is a standard method in factory conditions. Continuous research into the use of new additives and optimization of heat treatment of concrete makes it possible to increase its strength and hardening rate. Understanding the various factors influencing the hardening of concrete allows us to optimize its production and operation in various climatic conditions.

2. Methods

The production of the concrete mixture was carried out using the following materials:

- Cement I 42.5B, with specific effective activity of natural radionuclides for raw materials of 57 Bq/kg [11];

- Blast furnace slag crushed in a ball mill [12];

- Expanded polystyrene gravel, 2.5-5 mm fraction;

- Additives: air entrainment (Master Air 200) and superplasticizer (Master Rheobuild 270);

- Water.

The concrete mix was made by [13] (Figure 1).



Figure 1 – Concrete mix

The manufacturing technology is as follows: the dosed components were mixed in a container for 1 minute using an immersion mixer. After the introduction of additives, the mixture was mixed for another 1 minute, after which it was molded in molds with side dimensions of 10×10×10 cm [14]. A total of 30 samples were produced: 15 for each type of hardening (Figure 2).



Figure 2 – Polystyrene concrete samples for research

For a comparative analysis of the effect of heat treatment, a steaming chamber with a steam temperature from 18 to 100°C with a power of 4 kW was used. This chamber is designed to work in enclosed spaces with a temperature of at least + 5°C and humidity up to 80% [14] (Figure 3).



Figure 3 – Preparation of samples for steaming

Concrete steaming took place under the following conditions presented in Figure 4 below.

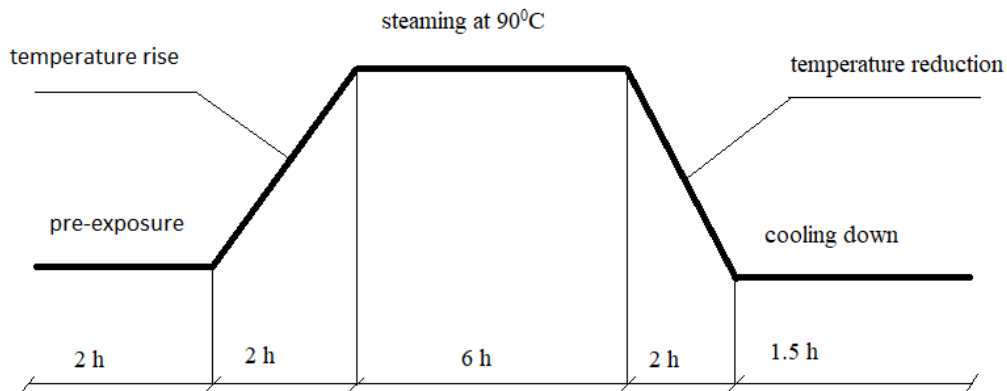


Figure 4 – Concrete heat treatment schedule

When steaming products, it should first withstand them and gradually increase the temperature, this will avoid cracks, then also gradually reduce the temperature. The entire steaming process takes approximately 13.5 hours. To determine the mechanical compressive strength, a hydraulic press for light concrete with a force of 10 tons was used (Figure 5).



Figure 5 – Mechanical compressive strength test

All samples were subjected to mechanical compressive strength tests at the ages of 1, 3, 7, 14, and 28 days.

3. Results and Discussion

Studies of the mechanical strength of polystyrene concrete hardened under normal conditions and in samples hardened in a steaming chamber at the ages of 1, 3, 7, 14, and 28 days were carried out. As can be seen from Figure 5, the heat treatment mode can significantly reduce the time of hydration and strength gain of finished products.

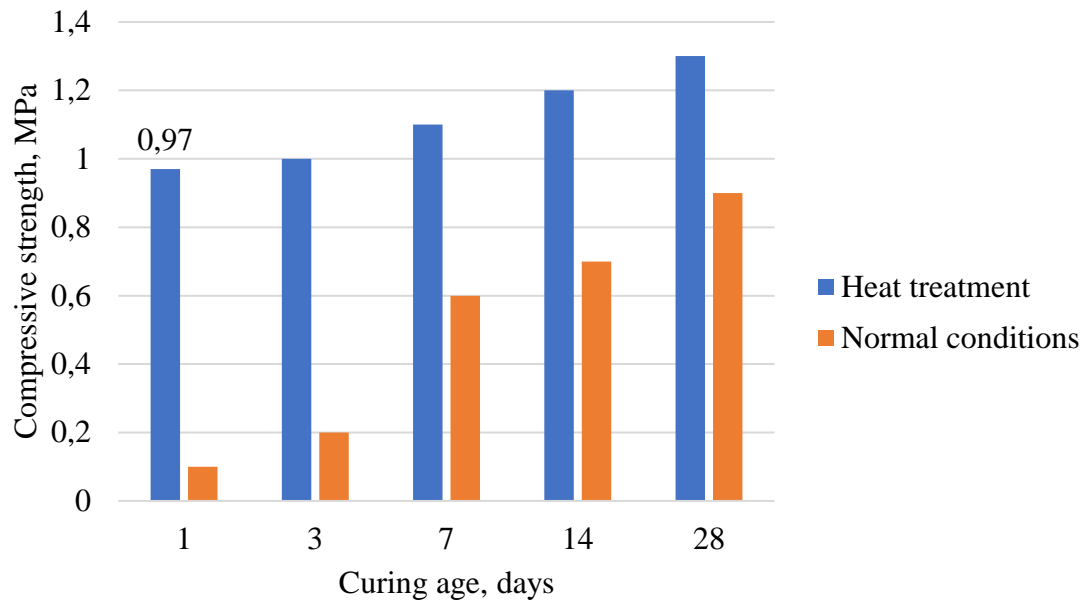


Figure 5 – Strengthening of samples

As shown above, the steamed polystyrene concrete exhibits consistently higher strength from day 1 through day 28 compared to regular polystyrene concrete, gaining 0.97 MPa strength for only 1 day of curing. The strength of heat-treated concrete turned 30% higher than that of concrete hardened under normal conditions. Figure 6 below shows the polynomial calibration dependence of the strength of concrete hardened during heat treatment and concrete hardened under normal conditions.

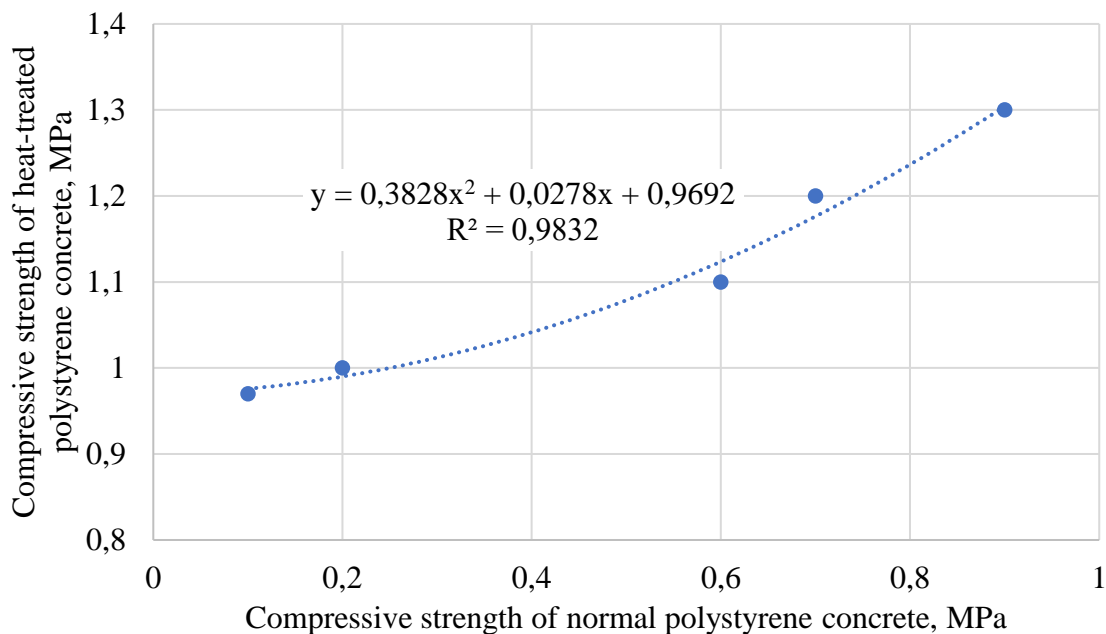


Figure 6 – Calibration dependence of the strengths of two types of samples

During the heating process of polystyrene concrete, air trapped in the mixture is released, as well as gaseous isopentane from expanded polystyrene. Air and isopentane form a vapor-air mixture in the liquid phase of the cement paste. At the initial stage of heating, this steam-air mixture is removed from the cement paste, creating channels for its entrainment. This occurs due to the expansion of the mixture and the presence of technological seams in the molds [15]. This is confirmed by a decrease in its density by 7% (Table 1).

Table 1 – Density of polystyrene concrete

Concrete hardening condition	The standard value of density, kg/m ³	Actual density, kg/m ³
Heat treatment	350-400	370
Normal conditions	350-400	398

The positive side of heat treatment is also manifested in the environmental component. The removal of the gas-forming agent (isopentane) from the mixture to the edges of the mold increases the environmental friendliness of the material [15].

4. Conclusions

1. The choice of heat treatment type depends on the thermal insulation material, its purpose, and the required properties. Incorrectly performed heat treatment can lead to deterioration of the properties of the material;

2. The heat treatment mode reduces the time of hydration and strength gain of finished products: the strength gain of concrete that has undergone heat treatment was less than 1 day, while concrete that hardened under normal conditions gained the required strength only for 28 days. The strength of warmed concrete is 30% higher than that of concrete hardened under normal conditions;

3. During the heating process of polystyrene concrete, isopentane is released from expanded polystyrene. At the initial stage of heating, this steam-air mixture is removed from the cement paste, creating channels for its entrainment. Therefore, polystyrene concrete is an environmentally safe material;

4. The density of polystyrene concrete after heat treatment is lower than that of polystyrene concrete hardened under normal conditions. This is due to the intense release of isopentane from polystyrene granules.

Thus, the density of polystyrene concrete after heat treatment is lower than that of polystyrene concrete hardened under normal conditions by 7%.

The results obtained will allow further research on the possibility of using the proposed composition of polystyrene concrete in the enclosing structures of large-panel housing, as well as on the effect of heat treatment on the properties of concrete.

References

- Heat-resistant porous high-temperature resistant concrete based on a boron-modified alumophosphate binder and man-made waste / V.M. Batrashov. — Penza, Russia: Penza State University, 2013. — 17 p.
- Prochnost' betona pri tverdenii v razlichnyh klimaticheskikh usloviyah / M.A. Rahimov, G.M. Rahimova, B.M. Toimbaeva, S.A. Zhautikova, E.K. Imanov // *Mezhdunarodnyj zhurnal prikladnyh i fundamental'nyh issledovanij*. — 2018. — No. 6. — P. 38–42.
- Issledovanie podvizhnosti tsementno-zolnyih past s giperplastifikatorami / M.A. Rahimov, Z.A. Suleymbekova // *Trudy Universiteta*. — 2020. — Vol. 79, No. 2. — P. 110–114.
- Development of the Composition of a Complex Modifier and Study of the Effect on the Physical and Mechanical Properties of Polystyrene Concrete / M. Rakhimov, G. Rakhimova, E. Tkach, V. Mudrenko // *Trudy Universiteta*. — 2022. — Vol. 86, No. 1. — P. 166–170. https://doi.org/10.52209/1609-1825_2022_1_166
- More Than Just Concrete: Acoustically Efficient Porous Concrete with Different Aggregate Shape and Gradation / L. Shtrepi, A. Astolfi, E. Badino, G. Volpatti, D. Zampini // *Applied Sciences*. — 2021. — Vol. 11, No. 11. — P. 4835. <https://doi.org/10.3390/app11114835>
- Mechanical Properties of Lightweight Aggregate Concrete Reinforced with Various Steel Fibers / K.-H. Yang, H.-Y. Kim, H.-J. Lee // *International Journal of Concrete Structures and Materials*. — 2022. — Vol. 16, No. 1. — P. 48. <https://doi.org/10.1186/s40069-022-00538-4>
- The Influence of Addition of Fly Ash from Astana Heat and Power Plants on the Properties of the Polystyrene Concrete / R. Niyazbekova, G. Mukhambetov, R. Tlegenov, S. Aldabergenova, L. Shansharova, V. Mikhailchenko, M. Bembenek // *Energies*. — 2023. — Vol. 16, No. 10. — P. 4092. <https://doi.org/10.3390/en16104092>
- Improvement of the concrete behaviour to sulphate corrosion using fly ash admixture collected by wet process / L.I. Diaconu, M. Rujan, A.C. Diaconu, A.A. Şerbănoiu, D.T. Babor, D. Plian // *IOP Conference Series: Materials Science and Engineering*. — 2020. — Vol. 789, No. 1. — P. 012018. <https://doi.org/10.1088/1757-899X/789/1/012018>

9. Method of calculating the modes of heat and moisture treatment of reinforced concrete products / K.V. Aksenchik, N.I. Shestakov // Bulletin of Cherepovets State University. — 2015. — No. 5. — P. 9.
10. Sustainable Development of Human Society in Terms of Natural Depleting Resources Preservation Using Natural Renewable Raw Materials in a Novel Ecological Material Production / C.M. Grădinaru, R. Muntean, A.A. Şerbănoiu, V. Ciocan, A. Burlacu // Sustainability. — 2020. — Vol. 12, No. 7. — P. 2651. <https://doi.org/10.3390/su12072651>
11. Portlandcement klasa 42,5 bystrotverdeyushij [Electronic resource] / CAC. — [2024]. — Mode of access: <https://cac.kz/en/site/product?serial=22&slug=portlandcement-klasa-425-bystrotverdeusij> (accessed date: 26.06.2024).
12. GOST 3476-74 Slags blast-furnace and electric-phosphoric granulated for manufacturing of cement. — 2021.
13. GOST R 51263-2012 Concrete with polystyrene aggregates. Specifications. — 2012.
14. GOST 10180-2012 Concretes. Methods for strength determination using reference specimens. — 2012.
15. Heat treatment of polystyrene concrete in three-layer panels / V.N. Kirichenko. — Moscow, Russia: Scientific research, design and Technological Institute of Concrete and reinforced concrete, 2009. — 76–77 p.

Information about authors:

Murat Rakhimov – Candidate of Technical Sciences, Associate Professor, Department of Construction Materials and Technologies, Abylkas Saginov Karaganda Technical University, Karaganda, Kazakhstan, m.rakhimov@kstu.kz

Galiya Rakhimova – Candidate of Technical Sciences, Associate Professor, Department of Construction materials and Technologies, Abylkas Saginov Karaganda Technical University, Karaganda, Kazakhstan, g.rakhimova@kstu.kz

Tatyana Samoilova – PhD Student, Department of Construction Materials and Technologies, Abylkas Saginov Karaganda Technical University, Karaganda, Kazakhstan, tanya.fedulova.18@mail.ru

Nurlan Zhangabay – Candidate of Technical Sciences, Associate Professor, Department «Architecture and urban planning», South-Kazakhstan University named after M. Auezov, Shymkent, Kazakhstan, nurlan.zhanabay777@mail.ru

Author Contributions:

Murat Rakhimov – methodology, analysis, interpretation, drafting, editing.

Galiya Rakhimova – methodology, analysis, interpretation, drafting, editing.

Tatyana Samoilova – concept, methodology, resources, data collection, testing, analysis, visualization, drafting, funding acquisition

Nurlan Zhangabay – methodology, analysis, interpretation, drafting, editing.

Conflict of Interest: The authors declare no conflict of interest.

Use of Artificial Intelligence (AI): The authors declare that AI was not used.

Received: 14.06.2024

Revised: 24.06.2024

Accepted: 25.06.2024

Published: 27.06.2024



Copyright: © 2024 by the authors. Licensee Technobius, LLP, Astana, Republic of Kazakhstan. This article is an open-access article distributed under the terms and conditions of the Creative Commons Attribution (CC BY-NC 4.0) license (<https://creativecommons.org/licenses/by-nc/4.0/>).



Study of the causes of the collapse of a high-rise chimney under conditions of long-term operation

Valentin Mikhailov¹, Serik Akhmediyev¹, Daniyar Tokanov¹, Nikolai Vatin²,
 Zhmagul Nuguzhinov¹, Askhat Rakhimov^{1*}

¹Faculty of Architecture and Civil Engineering, Abylkas Saginov Karaganda Technical University, Karaganda, Kazakhstan

²Peter the Great St. Petersburg Polytechnic University, St. Petersburg, Russia

*Correspondence: rakhimov.askhat@gmail.com

Abstract. This article analyzes the causes of the collapse of a high-rise chimney in Petropavlovsk. A study of the factors of long-term (over 60 years) operation of a high-altitude (H=150 m) chimney was carried out. The analysis of the constructive solution of the pipe was carried out, and the study of the operating conditions was performed. To theoretically assess the technical condition and stress-strain state factors (SSS) of the collapsed chimney, automated verification calculations were carried out based on the actual parameters and characteristics obtained during the last technical inspection. An automated verification calculation of SSS factors determining the bearing capacity of an object (its strength, rigidity, reliability, and durability) has been performed. Theoretically, the physical wear of the object has also been carried out. Based on the study of the available technical documentation and conducting a continuous, detailed instrumental examination of the facility, the expert organization established the significant causes that led to the pipe accident.

Keywords: chimney, industrial buildings and structures, technical inspection, reliability, calculations, physical wear, reliability and stability, defects and damages.

1. Introduction

Currently, the problem of ensuring the safe operation of energy facilities has become more acute. Accidents at Thermal Power Plants (TPPs) are associated with a high percentage of dilapidation of chimneys. The problems of destruction of buildings and structures are well studied, but there is little research in the field of safe operation and monitoring of the technical condition of chimneys. Chimneys of large height, are under continuous action of variable dynamic wind loads, and aggressive high-temperature gas flows [1, 2]. The collapse of chimneys is often associated with their wear and tear, lack of timely diagnostics of technical condition or repair, and the violation of operation and work in an aggressive environment. The articles [3-6] consider the main problems of chimney operation, as well as the issues of development and introduction into practice of a set of methods and measures for operational assessment of chimney wear [7].

No organization specializes in the design, construction, and inspection of chimneys in Kazakhstan today. Most industrial chimneys were built in the 50-70s of the 20th century, therefore, the issue of developing alternative renewable energy sources is rising more frequently [8]. The articles [9-11] discuss the problems that arise in the production of electricity using renewable energy sources. The design life of industrial structures is 50 years, and the periodicity of inspections should be performed at least once every 5 years [12, 13]. Regular inspection makes it possible to identify defects and damages, if detected, it is possible to stop operation and take measures to eliminate them. This

makes it possible to keep the structure safe and avoid human, environmental, and economic losses in the process of collapse.

Currently, to control the safety of industrial chimneys various methods are being developed. The articles [14-16] consider a method using an in-line autonomous apparatus capable of determining and registering defects in the lining of the chimney without disconnecting it from the operating boilers. Along with this, surveys of high-altitude chimneys at hazardous production facilities are carried out, so in [17-19] the main task of the survey is to determine the technical condition of the structure, assess the operational suitability and possible recommendations for bringing the object following the requirements of regulatory documentation.

Over the last decades, as a result of a sharp decline in industrial production due to the economic crisis in the country, the rupture of previously established relationships, and privatization of enterprises, significantly changed the modes of operation of industrial chimneys and weakened control over their technical condition, which adversely affects their strength characteristics. The accident that occurred at Petropavlovsk TPP-2 serves as a confirmation of this fact. In the third decade of March 2022, there was a partial collapse of the upper part of the pipe from 150 m to 97 m that destroyed several structures of nearby auxiliary and attached buildings and structures (smoke pump room, gas ducts) [20]. Therefore, this study aims to study the factors of the long-term (over 60 years) operation of a high-rise (H=150m) chimney in Petropavlovsk, as well as the causes that led to its collapse

2. Methods

Figure 1 presents a general view of the Petropavlovsk TPP-2 (Republic of Kazakhstan).



Figure 1 - General view of the chimney of Petropavlovsk TPP-2 after collapse

From the structural point of view, the object under study is a multilayer and variable thickness cantilever conical chimney with a length of about 150 m, the thickness of the chimney varies from

750 mm at the bottom to 160 mm at the top, the concrete of the chimney shaft corresponds to class B15 (grade M200 on Portland cement M400). The chimney is supported by a reinforced concrete round foundation with a diameter of 30.0 meters and a depth of 4.0 meters.

The chimney is three layers thick, the main (bearing) material is monolithic reinforced concrete, mineral wool mats overlapping the gap of 30-50 mm between the layers, and a lined layer made of ordinary bricks of 100 grade on the mortar of 25 grade.

The conditions of long-term operation are as follows: II wind region, flue gas temperature: 151-158°C (before gas cleaning), 76-85°C (after gas cleaning); flue gas humidity 8-10%; flue gas dew point temperature up to 30°C; atmospheric air temperature in the area of chimney location is: -43°C (in winter); +39°C (in summer); non-seismic terrain (up to 6 points); normative requirements for the 2nd limit state: allowable crack opening $s_{cr} = 0.1 \dots 0.2$ mm; displacement of the chimney top up to 1/75 of its height – 20 cm (from normative wind load).

The content of this article is devoted to the study of the technical causes that led to the emergency collapse of a part of the pipe based on the analysis of the results of a technical inspection conducted by a research and expert organization KazMIRR (Karaganda, Kazakhstan) [20].

The preliminary conclusion (without the results of the necessary verification calculations of the stress-strain state (SSS) of the chimney structures) of the experts is as follows. Partial collapse of the chimney shaft is a consequence of several factors superimposed during the period of long-term operation: low strength of concrete of some sections of the chimney (0.50...0.83% of the design grade); violation of the integrity of the lining of its part of the length and part of the thickness of the chimney, which significantly changed the state of the temperature field of the massif of the structure due to the inhomogeneity of the conditions of heat transfer and heat transfer, which resulted in a significant increase in the values of temperature displacements and directions; increase in the moisture content of the wall of the chimney, as well as to the reduction of the design thickness in certain sections of the pipe, which created conditions for a sharp increase in mechanical stresses as a result of their spontaneous redistribution and concentration in certain sections and joints as a result of the above unfavorable factors, the presence of which created their emergency combination, which sharply reduced the level of VAT of the object led to a partial collapse of the upper part of the pipe, in which the force factor (wind load pulsation) contributed to the conditions of reduction of bearing capacity parameters.

It should be noted that according to the data of the operators on the results of repeated technical inspections (1971, 1977, 1986, 2013), recommendations on the relevant repair works on the chimney were not carried out, moreover, according to the relevant norms the service life of such objects is about 50 years (the chimney under study has been operated for more than 60 years).

3. Results and Discussion

To theoretically assess the technical condition and VAT factors of the collapsed chimney, automated verification calculations were carried out according to the actual parameters and characteristics obtained during the last technical inspection, and the following results were obtained (Figure 2):

- 1.4 times underestimated the actual wind load, for which, for its time, this chimney was designed;
- the load-bearing capacity of the shaft on the first turbine of limit states, on which design sections are not provided (there is an excess of design resistance of concrete to compression);
- since the lining on the 10th section (in the area of +25.0m) is significantly disturbed (according to the results of the last inspection), the chimney shaft is in direct contact with flue gases, as a result of which the total stress from the force and temperature load amounted to 5.79MPa, which exceeds the design resistance of concrete in 5.1MPa (the increase in the total stress is due to the growth of temperature stress from 1.33MPa to 3.4MPa).

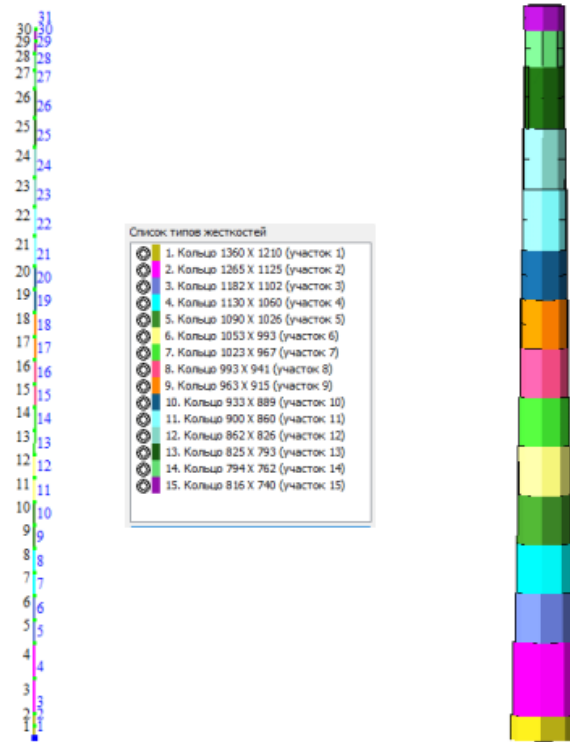


Figure 2 – Calculation diagram of the chimney

Thus, combining the analysis data of the preliminary conclusion on the technical condition of the chimney according to the results of the last (expert) inspection, which revealed a lot of defects and damages of quality and structures, basic materials (monolithic reinforced concrete, brick lining, mineral wool mats) with the results of automated verification calculation of VAT factors that determine the bearing capacity of the object (its strength, rigidity, reliability and durability). It should be noted that the main reason for the partial collapse of the chimney in Petropavlovsk is the physical deterioration caused by a long (excessive) period of operation (more than 60 years), a decrease in the amplitude of wind load during the design of the object according to outdated standards, the presence of defects in concreting and construction technology, failure to meet the deadlines for preventive maintenance and lack of a proper system of inspection and observation of the process of technical condition during the long period of operation of such a unique structure.

To assess the degree of physical deterioration on the technical condition of the object, let us determine theoretically the physical deterioration of the object by Eq. (1):

$$Q_f = 100 \times k_0^t \int 1.036^{t/5} dt \quad (1)$$

Where: the previous limit of integration "0" is taken as t=1 year; k=0,0168 (according to [21], Table 1; for the building of IV group of capitalization normative service life up to 50 years); t - 61 years (service life of the chimney at the time of the last technical inspection).

By (1) we obtain:

$$\begin{aligned} Q_f &= 5 \times 100 \times 0.0168 \times \frac{(1.036^{61/5} - 1.036^{1/5})}{\ln 1.036} = 8.4(1.5395 - 1.0071)/0.03537 \\ &= 8.4(0,5324)/0.03537 = 126.44 \\ Q_f &= 126.44\% > 100\%, \end{aligned}$$

i.e., the theoretical wear of the chimney in long-term operation (more than 61 years of operation) exceeds the limit (100%) wear.

The theoretical value $Q_f = 126.44\%$ corresponds to the established expert assessment of the technical condition of this object as "emergency" (or "unsuitable" for operation) ([22], Table 3, p.20).

Next, let's determine the statistical probability of further failure-free operation (FRO) of the system (chimney) beyond the service life (t = 61 years), established at the last technical inspection

(May 2022). We assume that the probability of failure follows the one-parameter exponential law of probability distribution [22], then we have:

$$p(t) = e^{-\pi t} \tag{2}$$

Where: t – operation period; π – failure rate.

Let's take theoretical time to first failure ($T_p=100$ years), then $[(\pi=1/T_p)=(1/100=0.01)]$.

1/year – failure rate.

Let's build a graph of "FRO" change according to Eq. (2) on the parameter "t" (Figure 3).

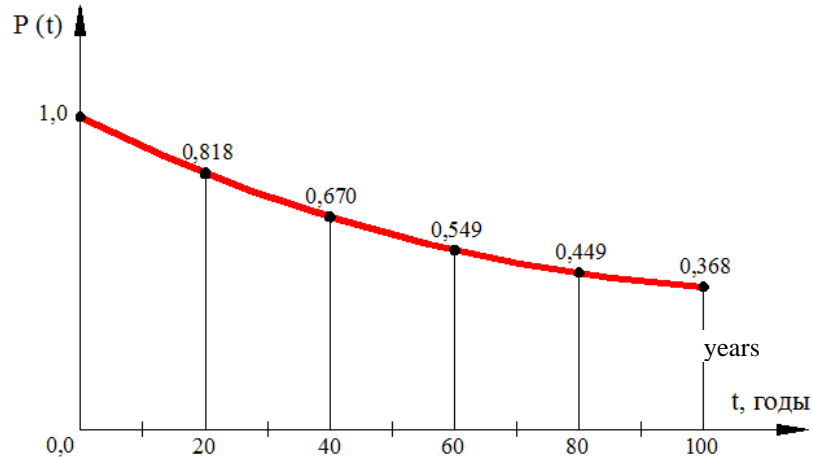


Figure 3 – Dependence of the "FFO" value on the parameter "t"

If we consider that the probability of failure-free operation (FFO) less than 67% is unacceptable from the point of view of reliability of further operation, then according to the graph in Fig. 1, the suitable service life of this chimney should not exceed 40 years. The actual service life of the chimney at the moment of the last technical inspection was more than 61 years, i.e., according to our research, the operation of the collapsed chimney should have been suspended more than 20 years ago.

In the course of the last technical inspection of the chimney, non-destructive methods of testing the strength of concrete R (MPa) with simultaneous determination by ultrasonic device UKS-MG4S of the speed of sound wave passing through the concrete material of the chimney sections were carried out by the device IPS-MG4.03. v (m/c).

At the same time, the results of tests in 38 sections for 78 control sections constituted a statistical sample with a spread of values in the range of $R = (8.8 \div 35.6)$ MPa; $v = (1703 \div 4669)$ m/c.

Based on these data, in this paper, we will conduct a bivariate regression analysis to establish a correlation relationship between the strength of the concrete of a chimney and the speed of sound traveling through the mass of its material [23, 24]. Further we denote: X_i – this R_i ; y_i – v_i . Table 1 shows the above concrete test results in the form of a two-dimensional statistical sample $N=78$, with all data pre-ranked in ascending order of their values by a constant step size in each of the accepted value ranges.

Table 1 – Concrete test results in 2D sample $N=78$

x_i , MPa \ y_i , m/s	$y_1=1000 \div 2000$	$y_2=2000 \div 3000$	$y_3=3000 \div 4000$	m_{xy}
$X_1=0 \div 10$	3	4	4	11
$X_2=11 \div 20$	4	21	12	37
$X_3=21 \div 30$	1	14	11	26
$X_4=31 \div 40$	–	–	4	4
m_{yy}	8	39	31	78

Let us divide the data of Table 1 into two separate worksheets: Table 2 – for parameters x_i ($i=1, 2, 3, 4$); Table 3 – for y_i ($i=1, 2, 3$).

Table 2 – X-parameters

x	n	xn	x^2n
10	11	110	1100
20	37	740	14800
30	26	780	23400
40	4	160	6400
Σ	78=N	1790	45700

Table 3 – Y-parameters

x	n	xn	y^2n
2000	8	16000	32000000
3000	39	11700	351000000
4000	31	124000	496000000
Σ	78=N	257000	879000000

Let's calculate the sampling parameters according to the table 2:

a) $\bar{x} = \sum xn / N = 1790 / 78 = 22.95$; $\bar{x}^2 = \frac{\sum x^2n}{N} = \frac{45700}{78} = 585.90$ – average values

b) Let's calculate the variance:
 $Dx = \bar{x}^2 - (\bar{x})^2 = 585.7025 - 526.7025 = 59$

c) Standard deviation:
 $\sigma_x = \sqrt{Dx} = \sqrt{59} = 7.68$

According to the Table 3:

a) $\bar{y} = 3294.87$; $\bar{y}^2 = 11269230.77$
 b) $Dy = 11269230.77 - (3294.87)^2 = 393284.23$
 c) $\sigma_y = \sqrt{393284.33} = 627.12$

Let's calculate the complex product of values ($n \times x \times y$) (Table 4) considering the Table 1 data.

Table 4 – Complex product of values ($n \times x \times y$)

x \ y	2000	3000	4000	m_{yi}
	10	60000	120000	
20	160000	1260000	960000	238000
30	60000	1260000	1320000	2640000
40	–	–	640000	640000
m_{xi}	280000	2640000	3080000	6000000

According to the data in Table 4, we calculate the value of \overline{xy} :

$\overline{xy} = \sum xny / N = 6000000 / 78 = 76923.08$

Then, using the data in Table 1, we will solve the following probabilistic questions:

1) Calculate the correlation relationship η_{xy} between the values of "x" and "y", by which we will determine the degree of their relationship with each other.

$$\int xy = \delta y / \delta y = \delta x / \delta x \tag{3}$$

Where: $(\delta x, \delta y)$ – "link" correlation coefficients.

If Eq. (3), in our case, yields a value (η_{xy}) close to one, then we can say that the correlation relationship between the statistical variables will be strong (i.e., they are strongly interrelated), otherwise, this relationship is weak.

2) Let's reveal the analytical dependence between the parameters x_i and y_i (Table 1) based on the available statistical sample, considering this dependence to be quadratic, according to Eq. (4).

$$y = a x^2 + b x + c \tag{4}$$

We determine the uncertain coefficients (a, b, c) in Eq. (4) by solving Eqs. (5-7).

$$\Sigma y = a \Sigma x^2 + b \Sigma x + c n \tag{5}$$

$$\Sigma x_i y_i = a \Sigma x^3 + b \Sigma x^2 + c \Sigma x \tag{6}$$

$$\Sigma x_i^2 y = a \Sigma x^4 + b \Sigma x^3 + c \Sigma x^2 \tag{7}$$

Let's determine the values $\bar{y}(x_i)$ (i=1, 2, 3, 4) according to Table 1.

$$\bar{y}(x_1=10) = \frac{\Sigma x_i y_i}{m_x} = \frac{32000+43000+44000}{11} = 3091.00$$

$$\bar{y}(x_2=20) = \frac{42000+213000+124000}{37} = 3216.22$$

$$\bar{y}(x_3=30) = \frac{13000+143000+114000}{26} = 2961.54$$

$$\bar{y}(x_4=40) = \frac{4 \cdot 4000}{4} = 4000.00$$

The following calculations are performed in Table 5 below.

Table 5 – Calculations

x	\bar{y}_k	m_x	$x m_x$	$x^2 m_x$	$x^3 m_x$	$x^4 m_x$	$\bar{y}_k m_x$	$x y m_x$	$x^2 y m_x$
10	3091.00	11	110	1100	11000	110000	34001	34010	3400100
20	3216.22	37	740	14800	296000	5920000	119000.14	2380003	47600000
30	2961.54	26	780	23400	702000	21060000	77000.04	2310001	69300030
40	4000.00	4	160	6400	256000	10240000	16000	640000	25600000
Σ	–	78=N	1790	45700	1265000	37330000	246001.18	5670014	145900130

Substituting the data (Table 5) into the Eqs. (5-7) (N=78) we get Eq. (8) below.

$$246001.18 = (45700)a + (1790)b + (78) c \quad (1/246001.18)$$

$$5670014 = (1265000)a + (45700)b + 1790 c \quad (1/5670014)$$

$$145900130 = (37330000)a + (1265000)b + (45700)c \quad (1/246001.18 \cdot 145900130)$$

or

$$1 = (0.1858)a + (0.00728)b + (0.000324)c$$

$$1 = (0.2231)a + (0.00806)b + (0.000316)c$$

$$1 = (0.2559)a + (0.00867)b + (0.000313)c \tag{8}$$

Solving Eq. (8) we determine the uncertain coefficients (a, b, c) in Eq. (9).

$$a = -1.62574 \quad b = 96.60 \quad c = 1848.19 \tag{9}$$

Substituting the values of Eq. (9) into the general Eq. (4) we obtain Eq. (10) below – the regression (statistical) relationship between concrete strength ($R_i=x_i$) (MPa) and sound propagation velocity in the concrete mass ($\vartheta_i = y_i$) (m/s).

$$y_i = 1.62574 x_i^2 + 96.6 x_i + 1848.19 \tag{10}$$

Eq. (10), obtained based on statistical processing of the results of in-situ tests of concrete sections of the chimney can be used also for other construction objects. Having determined the actual strength of concrete on this or that object of technical inspection, by Eq. (10) it is possible to determine analytically the speed of sound in concrete. The value v_i will be used in calculations of wave processes in various reinforced concrete structures.

4. Conclusions

In this paper, we analyzed and conducted an extensive study of the results of technical inspection of the structures of reinforced concrete high-rise chimney. The necessity of the inspection was caused by the fact that in March 2022 at the TPP-2 in Petropavlovsk there was a collapse of its upper part. The expert organization on the basis of the study of the available technical documentation and a comprehensive, detailed, and instrumental examination of the object established the significant causes that led to the failure of the chimney.

Taking into account verification calculations on the basis of generalized results of technical inspection, the following was established:

1. The object is in a significant degree of physical deterioration (service life at the time of the survey was more than 61 years) due to the factors of natural aging of materials that provide the necessary serviceability: concrete degradation, destruction of the integrity of the lining layer, as well as systematic force (wind load pulsation) and temperature (passing through the trunk of the pipe flue gases with increased temperature parameters of influence).

2. The absence of a system of superimposed control over the technical condition of structures by the operators, given that the high-altitude chimney is a complex and unique engineering structure, operated, moreover, in difficult climatic conditions (seasonal and daily temperature fluctuations), in the open atmosphere.

3. despite the recommendations of previous technical inspections (1971, 1977, 1986, 2013) the required preventive and mandatory repairs of the load-bearing parts of the facility were not performed on the chimney.

4. In-situ tests of the actual strength of concrete showed a wide variation of their indicators from 8.7 to 34.1 MPa, which indicates non-homogeneity of mechanical strength of different sections of the pipe, indicating unfavorable distribution of the main stresses along the design length of the structure.

5. Aging of the pipe structures confirmed the determination of the theoretical wear value, which amounted to more than 100%, while the calculation of theoretical wear established that 100% wear of the object should have occurred after 40 years of its operation (the actual period before the collapse - 61 years).

6. In this paper, based on in-situ tests by non-destructive methods of the results of concrete strength of the chimney sections, given by the expert organization during the last technical inspection, regression analysis of the relationship between the strength of concrete "R" and the speed of the sound wave through the sections of the chimney structure was performed; this analysis was performed with a statistical sample of data for 78 sections of the chimney. The analytical Eq. (10) obtained as a result of regression analysis allows determining the wave velocity of concrete of various structures at other construction sites, i.e., it is sufficiently universal.

7. In general, the outcomes and results of this study allow us to expand the scope of knowledge in the field of analyzing possible accidents of construction objects in order to develop a scientific and technical basis for preventing such collapses in the future.

References

1. Thermal and fluid dynamic behaviors in symmetrical heated channel-chimney systems / A. Andreozzi, B. Buonomo, and O. Manca // *International Journal of Numerical Methods for Heat and Fluid Flow*. — 2010. — Vol. 20, No. 7. — P. 811–833, <https://doi.org/10.1108/09615531011065584>
2. Dämpfung winderregter Schwingungen von Stahlschornsteinen in Gruppenanordnung / P. Adler, G. Hirsch // *Bautechnik* (Berlin, 1984). — 1986. — Vol. 53, No. 7. — P. 223–228.
3. Osnovnye problemy v ekspluatatsii dymovyh trub / Yablonko E.V // *Molodoy Uchenyi*. — 2011. — Vol. 9, No. 32. — P. 65–68.
4. Changes in the stress-strain state of soils with changes in humidity / A.S. Zhakulin, A.A. Zhakulina, A.U. Yessentayev, E. N. Abdygaliyev, and E.K. Imanov // *Smart Geotechnics for Smart Societies*. — 2023. — P. 1216–1221, <https://doi.org/10.1201/9781003299127-175>

5. Investigation of soils on the base of a reinforced concrete chimney / A. V. Filatov, A.S. Zhakulin, A.A. Zhakulina, P.A. Kropachev, S.S. Kuzmichev, and A.U. Yessentayev // in Smart Geotechnics for Smart Societies. — 2023. — P. 1432–1442, <https://doi.org/10.1201/9781003299127-213>
6. Improving the efficiency of power boilers by cooling the flue gases to the lowest possible temperature under the conditions of safe operation of reinforced concrete and brick chimneys of power plants / E. Ibragimov and S. Cherkasov // MATEC Web of Conferences. — 2018. — P. 1432–1442, <https://doi.org/10.1051/mateconf/201824507014>
7. Osnovnye problemy dymovyh trub i metody ih ustraneniya / Chistov R.A., Zhuravleva N.V. // Vestnik magistratury. — 2020. — Vol. 5-3, No. 104. — P. 1432–1442.
8. Unscented Kalman Filter for the identification of passive control devices // Research and Applications in Structural Engineering, Mechanics and Computation. — Florida, USA: CRC Press, 2013. — P. 59–60. <https://doi.org/10.1201/b15963-17>
9. Morphological comparative assessment of a rooftop solar chimney through numerical modeling / B. Zamora // International Journal of Mechanical Sciences. — 2022. — Vol. 227. — P. 107441. <https://doi.org/10.1016/j.ijmecsci.2022.107441>
10. Continuous power generation through a novel solar/geothermal chimney system: Technical/cost analyses and multi-objective particle swarm optimization / A. Habibollahzade, E. Houshfar, M. Ashjaee, K. Ekradi // Journal of Cleaner Production. — 2021. — Vol. 283. — P. 124666. <https://doi.org/10.1016/j.jclepro.2020.124666>
11. Recent Advancements in Ventilation Systems Used to Decrease Energy Consumption in Buildings—Literature Review / Ł. Amanowicz, K. Ratajczak, E. Dudkiewicz // Energies. — 2023. — Vol. 16, No. 4. — P. 1853. <https://doi.org/10.3390/en16041853>
12. Problemnye zadachi v upravlenii strategicheskimi riskami / V.A. Akatiev // Scientific notes of the RGSU. — 2010. — No. 7. — P. 115–119.
13. Issledovanie prichin avarijnosti promyshlennyh dymovyh trub / O.A. Karetnikova // Unikal'nye issledovaniya XXI veka. — 2015. — No. 8. — P. 67–71.
14. Vnutritrubnaya defektoskopiya funkcioniruyushchej promyshlennoj dymovoj trubyy / A.A. Aleksandrov, S.P. Sushchev, V.A. Akatiev, V.I. Larionov, E.V. Metelkin // Vestnik MGTU im. N.E. Baumana. Ser. Mashinostroenie. — 2016. — Vil. 6, No. 111. — P. 128–134.
15. Povyshenie effektivnosti kontrolya dymovyh trub s pomoshch'yu avtonomnogo apparata / A.A. Aleksandrov, V.A. Akatiev, V.I. Larionov, S.P. Sushchev, L.V. Volkova // Vestnik MGTU im. N.E. Baumana. Ser. Mashinostroenie. — 2017. — Vol. 1, No. 112. — P. 24–40.
16. Synchronized blasting demolition of workshop and chimney under complicated conditions / L.Z.S. Zou, J. Yang, Z. Y. Chen, C.L. He // Open Civil Engineering Journal. — 2017. — Vol. 11. — P. 726–736 <https://doi.org/10.2174/1874149501711010726>
17. Obsledovanie tekhnicheskogo sostoyaniya sooruzheniya na opasnom proizvodstvennom ob'ekte na primere kirpichnoj dymovoj trubyy vysotoj 45,0 metrov, ustanovlennoj na territorii kotel'noj / Yu.N. Barannikov, I.F. Safin, S.A. Davydenko, M.A. Kostrovsky, O.A. Bratygin // Aktual'nye problemy gumanitarnyh i estestvennyh nauk — 2015. — No. 12-2. — P. 14–19.
18. Predicting Service Life of Chimneys and Cooling Towers Based on Monitoring / M. Sykora, J. Markova, J. Mlcoch, J. Molnar, K. Presl // High Tech Concrete: Where Technology and Engineering Meet. — Cham: Springer International Publishing, 2018. — P. 1671–1679. https://doi.org/10.1007/978-3-319-59471-2_192
19. Selected problems of damage analysis of heat and power plant RC chimneys / M. Minch, A. Trochanowski // Prace Naukowe Instytutu Budownictwa Politechniki Wroclawskiej. — 1998. — Vol 70. — P. 179–180.
20. Tehnicheskoe zaklyuchenie. — Karaganda: KazMIRR, 2022. — 182 p.
21. Preduprezhdenie prezhdvremennogo iznosa zdaniy / G.A. Poryvay. — Moscow: Stroyizdat, 1979. — 284 p.
22. Veroyatnostnye metody v stroitel'nom proektirovanii / G. Augusti, A. Baratta, F. Casciati. — Moscow: Stroyizdat, 1988. — 576 p.
23. Prikladnoj regressionnyj analiz / N. Dreiper, G. Smit. — Moscow: Stroyizdat, 1988. — 576 p.
24. Prikladnaya statistika i osnovy ekonometriki / S.A. Ayvazyan, V.S. Mkhitaryan. — Moscow: Izdatel'stvo «Yuniti», 2001. — 107 p.

Information about authors:

Valentin Mikhailov – Candidate of Technical Sciences, Associate Professor, Department of Mechanics, Faculty of Architecture and Civil Engineering, Abylkas Saginov Karaganda Technical University, Karaganda, Kazakhstan, v.mihaylov@kstu.kz

Serik Akhmediyev – Candidate of Technical Sciences, Professor, Department of Mechanics, Faculty of Architecture and Civil Engineering, Abylkas Saginov Karaganda Technical University, Karaganda, Kazakhstan, a.ahmediev@mail.ru

Daniyar Tokanov – Candidate of Technical Sciences, Senior Lecturer, Department of Civil Engineering, Abylkas Saginov Karaganda Technical University, Karaganda, Kazakhstan, tokanov-daniyar@mail.ru

Nikolai Vatin – Doctor of Technical Sciences, Professor, Director of the Scientific and Technological Complex «Digital Engineering in Civil Engineering», Peter the Great St. Petersburg Polytechnic University, St. Petersburg, Russian Federation, vatin_ni@spbstu.ru

Zhmagul Nuguzhinov – Doctor of Technical Sciences, Professor, Department of Civil Engineering, Faculty of Architecture and Civil Engineering, Abylkas Saginov Karaganda Technical University, Karaganda, Kazakhstan, kazmirr@mail.ru

Askhat Rakhimov – PhD, Senior Lecturer, Department of Civil Engineering, Abylkas Saginov Karaganda Technical University, Karaganda, Kazakhstan, rakhimov.askhat@gmail.com

Author Contributions:

Valentin Mikhailov – testing, modeling, analysis.

Serik Akhmediyev – concept, methodology, resources.

Daniyar Tokanov – testing, modeling, analysis, visualization, interpretation, drafting.

Nikolai Vatin – methodology, analysis, visualization, interpretation.

Zhmagul Nuguzhinov – methodology, testing, modeling, analysis.

Askhat Rakhimov – testing, data collection, editing.

Conflict of Interest: The authors declare no conflict of interest.

Use of Artificial Intelligence (AI): The authors declare that AI was not used.

Received: 14.06.2024

Revised: 28.06.2024

Accepted: 29.06.2024

Published: 30.06.2024



Copyright: © 2024 by the authors. Licensee Technobius, LLP, Astana, Republic of Kazakhstan. This article is an open access article distributed under the terms and conditions of the Creative Commons Attribution (CC BY-NC 4.0) license (<https://creativecommons.org/licenses/by-nc/4.0/>).